ADVANCED MATERIALS
www.advmat.de

Transcriptome-Optimized Hydrogel Design of a Stem Cell Niche for Enhanced Tendon Regeneration

Wanqi Zhang, Ying Rao, Shing Hei Wong, Yeung Wu, Yuanhao Zhang, Rui Yang, Stephen Kwok-Wing Tsui, Dai Fei Elmer Ker, Chuanbin Mao, Jessica E. Frith, Qin Cao, Rocky S. Tuan, and Dan Michelle Wang**

Bioactive hydrogels have emerged as promising artificial niches for enhancing stem cell-mediated tendon repair. However, a substantial knowledge gap remains regarding the optimal combination of niche features for targeted cellular responses, which often leads to lengthy development cycles and uncontrolled healing outcomes. To address this critical gap, an innovative, data-driven materiomics strategy is developed. This approach is based on in-house RNA-seq data that integrates bioinformatics and mathematical modeling, which is a significant departure from traditional trial-and-error methods. It aims to provide both mechanistic insights and quantitative assessments and predictions of the tenogenic effects of adipose-derived stem cells induced by systematically modulated features of a tendon-mimetic hydrogel (TenoGel). The knowledge generated has enabled a rational approach for TenoGel design, addressing key considerations, such as tendon extracellular matrix concentration, uniaxial tensile loading, and in vitro pre-conditioning duration. Remarkably, our optimized TenoGel demonstrated robust tenogenesis in vitro and facilitated tendon regeneration while preventing undesired ectopic ossification in a rat tendon injury model. These findings shed light on the importance of tailoring hydrogel features for efficient tendon repair. They also highlight the tremendous potential of the innovative materiomics strategy as a powerful predictive and assessment tool in biomaterial development for regenerative medicine.

1. Introduction

Tendons, which are primarily composed of collagen fibers, play a crucial role in transmitting force from muscles to bones. Unfortunately, tendon injuries are common, and clinically repaired tendons still exhibit high failure rates (20–90%) with long-term functional deficiencies.[1,2] Cell therapy, particularly using mesenchymal stem cells (MSCs), has emerged as a promising approach to restore functional tendon tissue and treat tendon injuries, but is hampered by issues such as acute cell death, low cell retention and uncontrolled off-target tissue formation that may lead to poor clinical outcomes.[3–5] These critical issues must be addressed before MSC-based therapies for tendon repair can become a reality.

Next-generation materials, such as biofunctional hydrogels, hold significant promise to overcome the challenges encountered in stem cell therapy for tendon repair.[6] Hydrogels can be used to deliver cells into a defect where they provide an artificial cell niche that can "prime" encapsulated cells towards a desired "state of

W. Zhang, Y. Rao, S. H. Wong, Y. Wu, Y. Zhang, S. K.-W. Tsui, D. F. E. Ker, Q. Cao, R. S. Tuan, D. M. Wang
School of Biomedical Sciences
Faculty of Medicine
The Chinese University of Hong Kong
Hong Kong SAR, China
E-mail: tuanr@cuhk.edu.hk; wangmd@cuhk.edu.hk

W. Zhang, Y. Rao, Y. Wu, Y. Zhang, D. F. E. Ker, R. S. Tuan, D. M. Wang
Institute for Tissue Engineering and Regenerative Medicine
The Chinese University of Hong Kong
Hong Kong SAR, China

The ORCID identification number(s) for the author(s) of this article can be found under https://doi.org/10.1002/adma.202313722

DOI: 10.1002/adma.202313722

S. H. Wong, S. K.-W. Tsui, Q. Cao
Hong Kong Bioinformatics Centre
The Chinese University of Hong Kong
Hong Kong SAR, China

R. Yang
Department of Sports Medicine
Orthopedics
Sun Yat-Sen Memorial Hospital
Sun Yat-Sen University
Guangzhou 510120, China

D. F. E. Ker
Department of Biomedical Engineering
The Hong Kong Polytechnic University
Hong Kong SAR, China

D. F. E. Ker, R. S. Tuan, D. M. Wang
Center for Neuromusculoskeletal Restorative Medicine
Hong Kong Science Park
Hong Kong SAR, China

readiness" and induce robust and precise stem cell-mediated tendon differentiation, which has significant transformative potential in stem cell-based regenerative therapies.[7] In this respect, multiple tissue engineering strategies presenting independent or combinations of biochemical and biophysical biomaterial attributes, have been studied for tendon repair and regeneration. This includes natural or synthetic biomaterials,[8] bioinductive factors, such as growth factors and decellularized extracellular matrix (ECM),[9,10] mechanical loading,[11,12] microenvironmental stiffness,[13–15] and material topography,[16] to enhance tenogenesis. Among these strategies, the application of ECM has gained significant popularity in both clinical and research settings. Tendon ECM (tECM), in particular, possesses unique structural and compositional characteristics that demonstrate tissue-specific regenerative bioactivity, essential for maintaining tendon homeostasis and promoting effective tendon regeneration.[17,18] Our group has previously developed a urea-extraction protocol to prepare tECM, which offers several advantages compared to traditional acid pepsin extraction approaches.[18,19] Urea-extracted tECM retains a substantial number of key tendon ECM components and demonstrates robust, tendon-specific bioactivity on human adipose-derived stem cells (hASCs), making it a promising biochemical factor for enhancing stem cell tenogenesis.[18–20] Furthermore, mechanical loading plays a fundamental role in every stage of the musculoskeletal system's lifespan.[21,22] In particular, the application of external mechanical stimulation, such as uniaxial cyclic loading within the physiological strain range of 3 to 10%, successfully replicates the strains experienced by tendons.[23,24] This mechanical loading, when combined with bioinductive factors like growth factor and ECM, has proven to be an effective approach in promoting tenogenesis across various systems.[25–28] However, the specific importance and optimal combined effects of these cues in modulating stem cell-mediated tendon induction remain unclear, presenting challenges in the rational utilization of hydrogel design parameters. As a result, conventional approaches to biomaterial development require intuitive tailoring of multiple parameters with long development cycles and high expenses. Furthermore, these endeavors demand significant efforts to inform and optimize strategies for tendon repair.[29,30]

Conventional approaches to evaluate a newly developed biomaterial involve sequential characterizations such as ex vivo, in vitro, as well as preclinical and clinical in vivo assessments.[31] For example, early studies typically employed conventional biochemical, histological, and molecular biology techniques such as quantitative polymerase chain reaction (qPCR) and microarrays to gauge the impact of biomaterials on cells. However, it is very challenging to accurately assess biomaterial bioactivity in terms of tenogenic cell fate.[32] This is due in part to the limited number of genes for defining the tendon phenotype, e.g., scleraxis (*SCX*), tenomodulin (*TNMD*), mohawk (*MKX*), and fibromodulin (*FMOD*).[33,34] Additionally, these markers are also expressed in other tissues and thus not truly unique to tendons, e.g., *SCX*, despite being an important tendon transcription factor, is also expressed in both heart and ligaments.[35,36] This indicates that tendon phenotype cannot be well defined by the use of a few "tendon" genes,[37] possibly leading to aberrant phenotypes and undesired side effects or impaired function. Additionally, by exclusively focusing on the tendon phenotype, biomaterial scientists may inadvertently overlook other crucial biological activities (e.g., proliferation, osteogenesis, senescence) involved in tendon healing. For example, despite the promising results of using collagen hydrogel seeded with MSC for rabbit tendon repair, there have been reports of ectopic bone formation in the tendon defect sites.[38] Also, an allogenic adipose cell therapy (ALLO-ASC Injection, Bukwang Pharmaceuticals) that used fibrin hydrogel to load adipose-derived mesenchymal stem cells (ASCs) for treating extensor tendinosis, was terminated in phase 2 clinical development (NCT03449082). These detrimental outcomes highlight the limitations of solely relying on niche-mimetic biomaterials to guide stem cell differentiation, although promising, can often be largely unpredictable and uncontrolled.[39] Therefore, there is a critical need to develop an in-depth assessment and predictive tool that can help comprehensively understand the contributions of various material features on targeted cell behaviors. This would enable more effective guidance in the design of materials for stem cell-mediated tendon repair.

In recent years, "materiomics" has emerged as a cutting-edge approach that leverages data science with biological omics data (such as genomics, transcriptomics, proteomics, metabolomics), material properties, advanced manufacturing techniques, and artificial intelligence (AI) tools. This integrated approach can be applied throughout the entire therapeutic development pipeline to generate highly tailored and efficacious biomaterials with significant translational potential.[30,40] In particular, materiomics advancements using RNA-seq have given researchers the ability to systematically visualize global transcriptomic responses to biomaterials, providing critical mechanistic insights into cellular processes and signaling pathways.[41] Such efforts include studies that characterized impact of biomaterial design, such as hydrogel viscoelasticity, stiffness, and adhesion ligands on gene expression using PCR or RNA-seq.[42–44] Additionally, machine learning as a branch of AI and computer science has emerged as an efficient strategy to predict stem cell lineage fate prediction and provide preliminary biomaterial functional evaluation.[45] However, the application of transcriptomics analysis and machine learning in

D. F. E. Ker, R. S. Tuan, D. M. Wang
Department of Orthopaedics and Traumatology
Faculty of Medicine
The Chinese University of Hong Kong
Hong Kong SAR 999077, China
C. Mao
Department of Biomedical Engineering
The Chinese University of Hong Kong
Hong Kong SAR, China
J. E. Frith
Materials Science and Engineering
Monash University
Clayton 3800, VIC, Australia
J. E. Frith
Australian Regenerative Medicine Institute
Monash University
Clayton 3800, VIC, Australia
J. E. Frith
Australian Research Council Training Centre for Cell and Tissue Engineering Technologies
Monash University
Clayton 3800, VIC, Australia

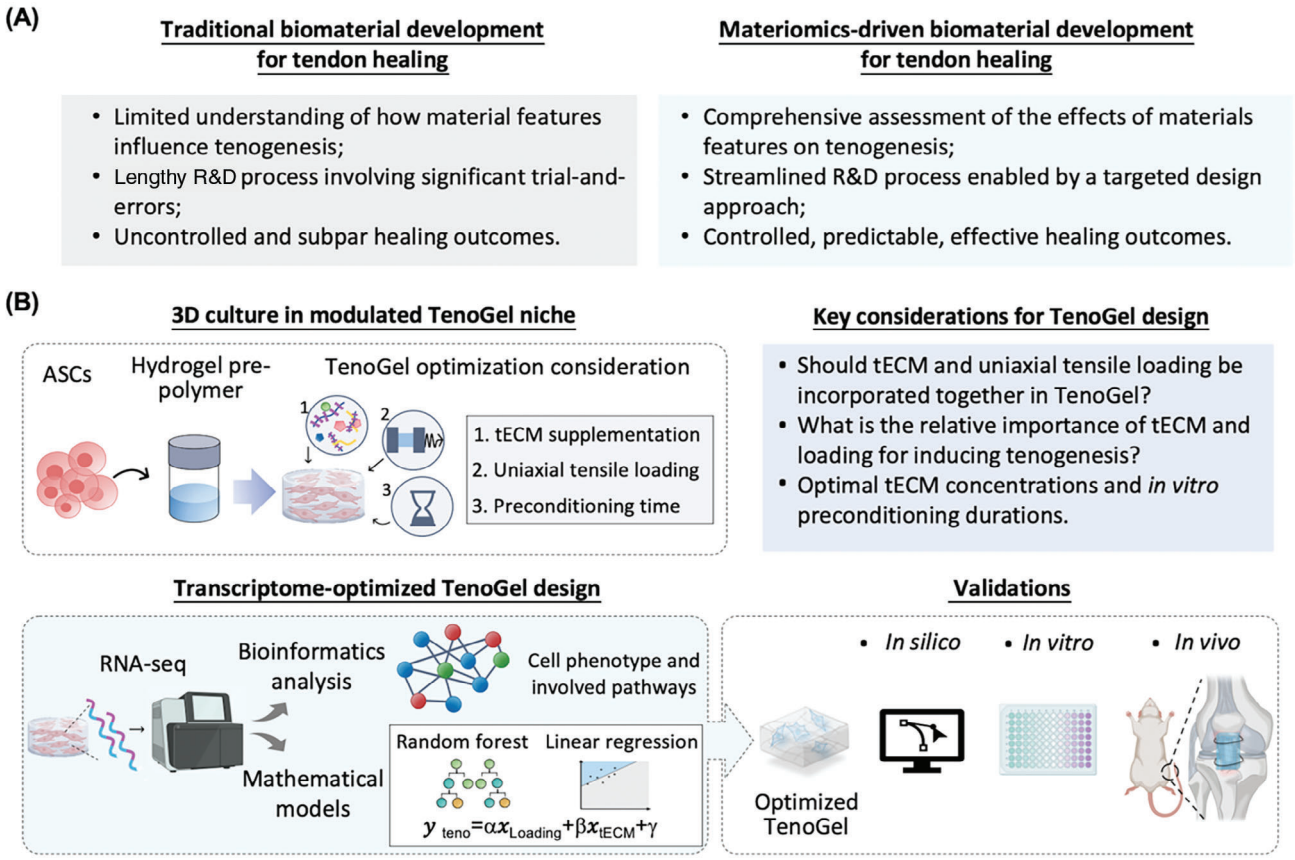

Scheme 1. Study objectives and overview. A) Study objectives: The limited understanding of how material niche properties influence cellular responses has resulted in lengthy development cycles and unpredictable and uncontrolled healing outcomes. To address this challenge, "materiomics" has emerged as a powerful, data-driven tool that can be utilized throughout the entire biomaterials development pipeline, which overcomes the limitations of traditional empirical methods and enables the rational engineering of biomaterials with enhanced therapeutic efficacy. B) Study overview: Our materiomics strategy is based on our in-house RNA-seq data and consists of two major components. First, we use bioinformatics to provide a mechanistic investigation into the cellular responses to different hydrogel features. Second, we develop mathematical modeling to quantitatively assess and predict the tenogenic effects of the hydrogel design. The knowledge generated from the materiomics assessment will ultimately lead to a highly effective, targeted approach for TenoGel design and improve its efficacy for stem cell-mediated tendon regeneration.

biomaterials design has not been extensively applied to define tendon phenotypes, which limits our understanding of the relative importance and contribution of the biological, biochemical, and biophysical features of tendon biomaterials. Therefore, implementation of an interdisciplinary methodology that converts an omics-based readout into a comprehensive and functional cellular assessment tool fulfills a crucial need for optimizing the design of next-generation bioactive tendon materials.[30,40]

In this study, to augment hydrogel-assisted stem cell tendon regeneration, we have established a tendon-mimetic hydrogel niche, TenoGel, as a technology platform that allows systematic modulation of specific tendon niche aspects such as tECM and uniaxial tensile loading based on their established roles in tenogenesis as well as our prior experiences.[9] Concurrently, we have developed an innovative RNA-seq-based materiomics strategy that contains two major components: bioinformatics analysis and mathematical modeling. This integrated approach represents a significant departure from traditional methods of hydrogel development, which have typically relied on empirical testing and trial-and-error optimization. The bioinformatics analysis aims to provide in-depth mechanistic insights into the transcriptomic responses of ASCs to single and combinations of various TenoGel design parameters. In parallel, the mathematical modelling component takes a quantitative approach to assess and predict the tenogenic effects of the hydrogel design (**Scheme 1**). For TenoGel design space, there exist a multitude of design parameters, which can be arranged in various permutations and combinations. These include but are not limited to number of encapsulated cells, material composition (ratio and/or concentrations of gelatin methacryloyl (GelMA) and alginate), incorporated tECM concentration, tensile loading settings (frequency, strain, strain rate, etc.), and in vitro pre-conditioning duration (total pre-conditioning duration, pre-conditioning interval/duration per day). In this study, our design considerations focused on: (1) determining whether tECM and uniaxial tensile loading should be employed separately or in combination within TenoGel, and elucidating their relative importance in inducing tenogenesis and potential mechanisms of action; (2) elucidating the optimal concentrations of tECM; (3) identifying the optimal duration (i.e., day 6, day 10, or day 21) for in vitro pre-conditioning of ASCs

in TenoGel. Herein, we show that our tendon materiomics approach can be used as a predictive and assessment tool to aid the development of highly bioactive TenoGel, with demonstrated tendon healing efficacy in vitro and in a rat patellar tendon injury model. Notably, in vivo studies using the optimized TenoGel formulations identified by our materiomics data showed native tendon-like tissue healing and avoided undesired ectopic ossification. This proof-of-concept demonstration of our materiomics approach provides new insights into cell niche parameters in tenogenesis, which have informed the development of an optimized biomaterial for stem cell-mediated tendon repair. Moreover, this systematic, data-driven understanding is crucial for biomaterial development, as it allows us to strategically allocate our efforts and resources towards a highly targeted approach for biomaterial design, which has significant potential for translation to broader applications in regenerative medicine.

2. Results

2.1. GelMA/OA Exhibited Excellent Material Features as an Appropriate Biomaterial Base for Developing TenoGel

To establish a robust platform (TenoGel), within which specific factors (i.e., tECM and uniaxial tensile loading) could be modulated to isolate the impact of niche cues, it was first necessary to develop a hydrogel biomaterial with specific features, including biocompatibility, robust mechanical features, and slow degradation. The purpose of incorporating these features was to ensure that the hydrogel provides adequate physical protection and sustains the intended duration of tensile loading during the in vitro pre-conditioning of ASCs. The base of the TenoGel was formed using GelMA and alginate in view of their frequent use in tissue engineering studies. In particular, the TenoGel system was inspired by a previously reported interpenetrating network (IPN) hydrogel gelatin methacryloyl/oxidized alginate (GelMA/OA),[46] which showed mechanical toughness and slow degradation needed to withstand the dynamic mechanical environment required during in vitro pre-conditioning and long-term in vivo regeneration of injured tendons. We first systemically characterized the molecular structure/functional groups, biomechanical properties, hydrogel pore structure, degradation rate, and cytocompatibility of the GelMA/OA system.

GelMA/OA was synthesized by forming Schiff base linkages between the aldehyde groups of OA and the amine groups of GelMA, along with ionic cross-linking of OA and photo-cross-linking of GelMA (**Figure 1A**). Fourier transform infrared spectroscopy (FTIR) analysis revealed a characteristic peak at 1626 cm^{-1} corresponding to C═N bonds, which demonstrated the Schiff base linkage formation (Figure 1B). Tensile tests showed that compared to the GelMA control hydrogel (tensile modulus, 44 ± 16 kPa; ultimate tensile stress, 30 ± 12 kPa), GelMA/OA exhibited a remarkable enhancement in mechanical strength, withstanding a maximum strain of ≈54.2% and exhibiting 4.4- and 3.4- fold improvements in tensile modulus (236 ± 19 kPa) and ultimate tensile stress (133 ± 38 kPa), respectively (Figure 1C). With regard to the stability of the hydrogel, the modulus of GelMA/OA remained relatively stable for 14 days of ex vivo incubation in PBS, with an initial modulus of 210 ± 18 kPa, but significantly decreased to ≈186 ± 18 kPa after 21 days incubation ($p < 0.01$). Similarly, the ultimate tensile stress of GelMA/OA significantly decreased to 82 ± 19 kPa after 14 and 21 days of incubation in PBS. Ex vivo degradation tests showed that GelMA/OA exhibited a controlled mass loss of ≈43% over an 8-week period (Figure 1D). Scanning electron microscopy (SEM) images confirmed the preservation of the open porous structures and pore morphology even after 8-week incubation in PBS, indicating stable hydrogel integrity (Figure 1D). Additionally, despite being mechanically tough, GelMA/OA facilitated cell spreading (as early as day 6), viability, and proliferation of hASCs as evidenced by LIVE/DEAD and MTS assays (Figure 1E).

Together, these findings provide collective evidence that the base of the TenoGel, an IPN-structured GelMA/OA hydrogel, exhibited robust mechanical properties, slow degradation, and cytocompatibility that supported the rapid spreading and viability hASCs. These material features validated it as an appropriate base for developing TenoGel, enabling subsequent systematic materiomics analysis.

2.2. TenoGel as a Tendon-Mimetic Hydrogel Niche Allows Systematic Modulation of tECM and Uniaxial Tensile Loading

While there are numerous niche features that can potentially influence ASC behavior, our focus in designing TenoGel has been centered on two key features: treatment with pro-tenogenic urea-extracted tECM and exposure to dynamic uniaxial tensile loading, based on our prior experience and understanding of their significance in regulating ASC tendon differentiation (**Figure 2A**).[18,19,25,47] The first objective was to evaluate the potency of tECM as a pro-tenogenic factor, as well as to assess the incorporation and release of tECM from GelMA/OA. Our data showed that tECM batch-to-batch variability was low (Figure S1A, Supporting Information) and when used as a medium supplement (1 mg mL^{-1}, 10% in growth medium) for 2D culture, tECM induced robust tenogenic differentiation of hASCs based on established tenogenic markers using immunofluorescence staining (Figure S1B, Supporting Information). Moreover, tECM can be successfully incorporated into GelMA/OA for hydrogel synthesis. tECM could be used at its highest protein concentration of 1.5 mg mL^{-1} in the hydrogel, which represents the upper limit of tECM solubility, without interfering with hydrogel polymerization (data not shown). Additionally, when encapsulated in GelMA/OA hydrogel, tECM exhibited sustained release kinetics, with an initial 25% burst release over the first 24 h followed by gradual release reaching ~52% of the initial loaded proteins by day 14 (Figure 2B).

We next investigated whether the GelMA/OA hydrogel can effectively transmit tensile loads to the encapsulated cells. To apply uniaxial tensile loading, hydrogel constructs were mounted onto a commercial bioreactor (CellScale T6) and subjected to physiological loading regimens, 8% strain, 0.5 Hz, and 6 h per day, as previously reported.[23,24] To examine the effects of loading on hASCs in TenoGel, finite element analysis (FEA) was performed (Figure 2C). The analysis revealed that under uniaxial tensile loading (8% strain), the hydrogel experienced a uniform mechanical environment, except in the areas near the free edges of the interface between the clamps and the hydrogel (ROI 1, Figure 2C). In these regions, stress concentrations were ob-

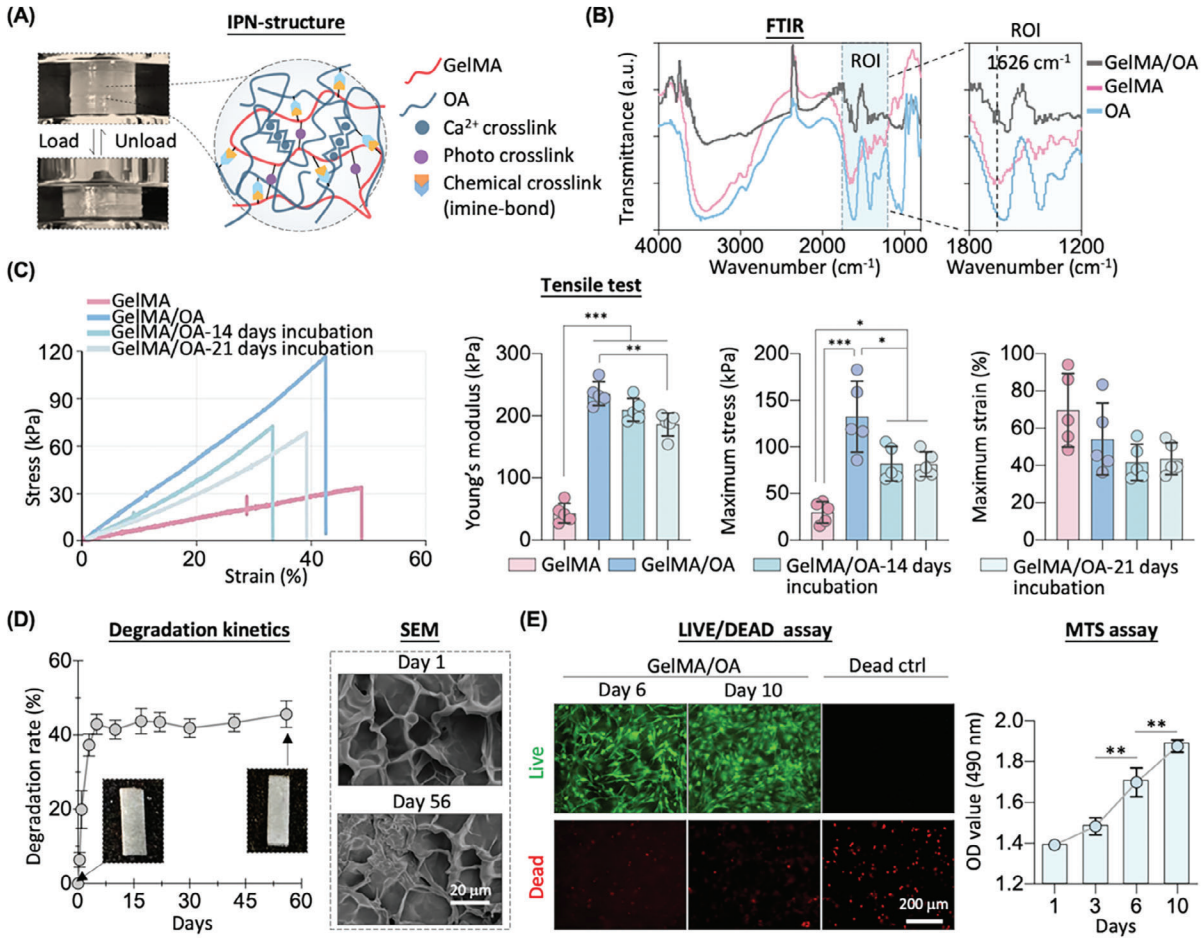

Figure 1. Ex vivo characterization of GelMA/OA hydrogel. A) IPN-structured hybrid hydrogel: the schematic illustrates the triple network formed in GelMA/OA hydrogel, consisting of Ca^{2+} cross-linked OA, covalent cross-links in photocured GelMA, and the imine bond formed between GelMA and OA based on Schiff base reaction. Digital images demonstrated the highly elastic property of the ADA/GelMA. B) FTIR: FTIR spectra of GelMA/OA hydrogel and its individual components, indicated the formation of imine-bonds ≈1690–1640 cm^{-1}. C) Tensile test: representative stress-strain curves and tensile tests showed the robust tensile attributes of the GelMA/OA hydrogel (freshly prepared and after PBS incubation at indicated time points), which were superior to those of GelMA hydrogel. $n = 5$; mean ± SD; *, $p < 0.05$; **, $p < 0.01$; ***, $p < 0.001$. D) Degradation kinetics: the degradation curve and representative SEM images after 1 day and 56 days of incubation in PBS, demonstrated the slow degradation rate and the maintenance of the homogeneous, porous structure of the GelMA/OA hydrogel. $n = 5$; mean ± SD. E) Cell viability test: representative LIVE/DEAD images and MTS assay of encapsulated hASCs cultured 6- and 10-days showing cells have a high rate of viability and proliferation in GelMA/OA hydrogel and exhibiting elongated cell bodies. Green, calcein-labeled live cells; red, EthD-1-labeled dead cells. $n = 3$ biological replicates; mean ± SD; **, $p < 0.01$.

served, which may cause uneven stimulation of the embedded cells. To ensure consistency in evaluation, subsequent analyses therefore focused on samples subjected to loading from the central region of the hydrogel (ROI 2, Figure 2C).

Moreover, as TenoGel was designed as a technology platform for studying the role of tECM and tensile loading in the cell niche for promoting tenogenesis, we conducted a primary examination of the viability, adhesion, and alignment of hASCs encapsulated within TenoGel over a 21-day pre-conditioning period under static culture/Gel (Ctrl), uniaxial loading alone/TenoGel (Loading), tECM alone/TenoGel (tECM), and tECM with uniaxial loading/TenoGel (tECM+Loading) (Figure 2D). This investigation was important as tough hydrogels are usually unfavorable for cell adhesion and spreading,[48–50] and they may lead to stress shielding effects that prevent hASCs from experiencing the intended tensile loading stimulation generated by our tensile loading bioreactor.[51,52] Our data showed that hASCs exhibited high viability in all conditions over a period of 21 days as evidenced by LIVE/DEAD staining (Figure 2D). Additionally, F-actin and DAPI nuclear staining revealed that TenoGel under uniaxial tensile loading, with or without tECM supplementation, displayed a greater number of cells with an organized arrangement of cytoskeletal actin filaments compared to the randomly oriented actin observed in the static groups at all timepoints (Figure 2E). Consistent with cytoskeletal changes, nuclei in the static groups appeared rounded or slightly elongated, while nuclei seen in constructs subjected to loading stimulation displayed a more oval-shaped and elongated appearance (Figure 2E). Additionally, we assessed the microscale mechanical properties of each TenoGel group using nanoindentation, which provides insights

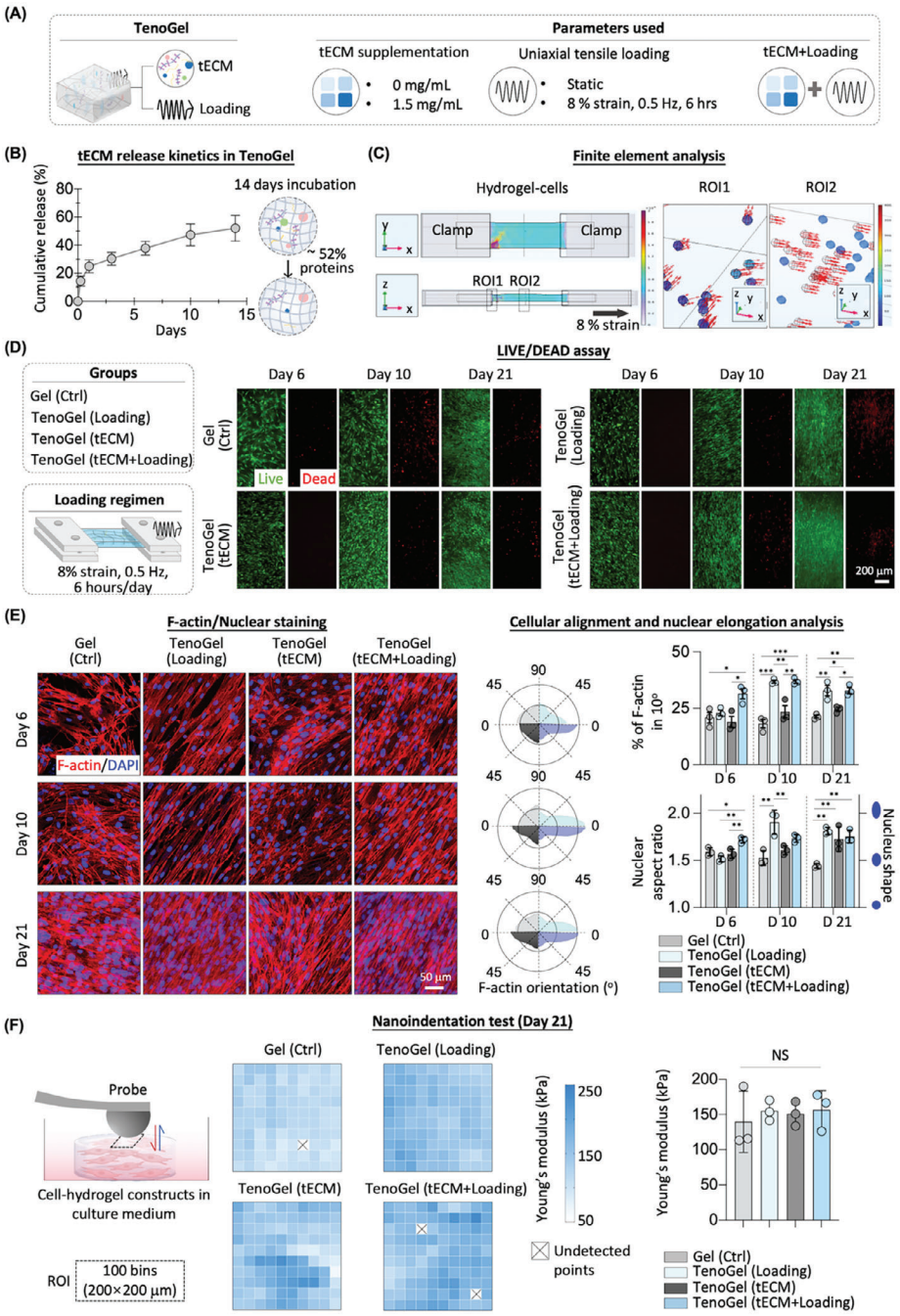

Figure 2. Characterization of tECM and uniaxial tensile loading as two key features within TenoGel. A) Study overview: schematic of TenoGel setup and parameters of tECM concentration and loading regimens. B) tECM release kinetics: the release curve showed the controlled release of tECM from TenoGel, with ≈52% of the proteins released after 14 days of incubation in PBS. $n = 5$; mean ± SD. C) FEA: the representative model demonstrated the stress distribution of cell-hydrogel constructs subjected to uniaxial tensile loading (8% strain) using a bioreactor. The simulated stress distribution within the hydrogel demonstrated a highly uniform mechanical field in the central region, with the exception of the areas near the clamps. Meanwhile, the cells located in the edge region (ROI 1) and middle region (ROI 2) experienced distinct loading effects (surface color map: principal stress intensity; red arrows: principal stress direction). To ensure consistency in evaluation, samples from the central region of the hydrogel were selected for subsequent analyses. D) LIVE/DEAD assay: representative LIVE/DEAD images showed high viability of hASCs in various TenoGel on days 6, 10, and 21. $n = 3$ biological replicates; Left panel: green, live cells; right panel: red, dead cells. E) F-actin/Nuclear staining: representative images and quantitative analysis of cytoskeletal structure and nucleus shape illustrated the alignment and elongation of hASCs under uniaxial tensile loading in TenoGel (red, F-actin; blue, nuclei). $n = 3$ biological replicates; mean ± SEM; *, $p < 0.05$; **, $p < 0.01$; ***, $p < 0.001$. F) Microscale mechanical characterization of TenoGel by nanoindentation. Indentation maps were generated from 100 points within a 200 μm × 200 μm area, demonstrating that all TenoGel constructs exhibited similar Young's modulus at day 21. These findings indicate that the incorporation of tECM and the application of uniaxial loading had no significant impact on the overall mechanical properties of TenoGel during the culture period. $n = 3$ biological replicates; mean ± SD; not significant (NS), $p > 0.05$.

into the localized mechanical microenvironment experienced by the cells. After 21 days of in vitro culture, all TenoGel constructs exhibited similar Young's modulus, averaging ≈140 kPa. This suggested that incorporation of tECM and the application of uniaxial loading did not significantly affect the overall mechanical properties of TenoGel throughout the culture period. As a result, the effect of the matrix modulus on the cells did not vary significantly among the different TenoGel groups (Figure 2F).

Together, these findings demonstrate that various forms of TenoGel were cytocompatible and could support hASC preconditioning in vitro for at least 21 days. Furthermore, when subjected to uniaxial tensile loading, encapsulated hASCs within TenoGel experienced tensile loading stimulation, resulting in alignment and elongation of both cell and nuclei parallel to the loading direction. These findings demonstrated successful establishment of TenoGel with modulated tECM and uniaxial tensile loading, which was further explored in downstream materiomics analysis.

2.3. Transcriptional Landscape of hASC Tenogenesis was Highly Correlated with TenoGel Niche Features

Despite the recognized significance of tECM and tensile loading in promoting tenogenesis, there remained a notable gap in our understanding of their relative importance and contribution, as well as the optimal combination of these parameters necessary to induce robust tenogenesis. Therefore, to gain insights into the interactions between tECM and tensile loading within the TenoGel, we used RNA-seq to analyze the transcriptional response of hASCs to the four distinct combinations of TenoGel features (Gel (Ctrl), TenoGel (Loading), TenoGel (tECM), and TenoGel (tECM+Loading)) on days 6, 10, and 21 (**Figure 3**A).

Principal component analysis (PCA) was conducted to investigate the overall transcriptional changes in hASCs exposed to the varying combinations of tECM and mechanical loading (Figure 3B). This revealed that the primary source of transcriptional variation was not tied to one specific material parameter, but the first principal component (PC1) effectively captured the dissimilarities between "Gel (Ctrl)" and other groups. Additionally, PCA conducted at each time point revealed that the differences caused by the group with both tECM supplementation and mechanical loading exhibited the greatest dissimilarity compared to the other groups on day 10. However, by day 21, the TenoGel samples supplemented with tECM alone and those supplemented with both tECM and mechanical loading clustered together, indicating a similar response over time, as depicted in Figure S2 (Supporting Information). To further elucidate the genes contributing to this divergence, we identified the genes with the highest contributions to PC1, which notably, were several well-established tendon markers such as *SCX, COMP, POSTN, COL11A1*, and *ELN* (Figure 3B). Subsequently, we performed a pairwise comparison to identify differentially expressed genes (DEGs) between groups. Overall, the TenoGel (tECM+Loading) group exhibited the highest number of DEGs compared to Gel (Ctrl) at each time point, far exceeding the DEGs generated by tECM alone and loading alone in the decoupled gene sets. (Figure 3C). Of these, several well-established tendon markers, e.g., *COL11A1, COMP, ELN, POSTN*, and *SCX*, had increased gene expression in TenoGel (tECM+Loading) compared to Gel (Ctrl) (Figure 3D). Taken together, these findings suggest that the combined effects of tECM supplementation and uniaxial tensile loading induce robust and distinctive transcriptional changes in hASCs, which were strongly associated with tenogenic genes.

We next focused on cell phenotype characterization, particularly regarding tenogenic and osteogenic differentiation. This is crucial because a clinical concern associated with stem cell-based tendon repair is unwanted osteogenesis leading to ectopic bone formation that may cause pain and joint dysfunction.[32,53] Heatmap analysis of selected lineage signature genes suggested that TenoGel groups (i.e., TenoGel (tECM), TenoGel (Loading), and TenoGel (tECM+Loading)) demonstrated enhanced tenogenesis over time compared to Gel (Ctrl) group. Notably, the TenoGel (tECM+Loading) exhibited the most pronounced tenogenic effect (Figure 3E). However, selected osteogenic markers also indicated that TenoGel (Loading) demonstrated stronger osteogenic differentiation rather than tendon differentiation, suggesting that the effects of loading were not specific to tenogenesis (Figure 3E). Moreover, quantitative analysis using single-sample gene set enrichment analysis (ssGSEA) also revealed similar findings in that: TenoGel (tECM+Loading) showed significantly higher tenogenesis ssGSEA scores compared to Gel (Ctrl) and TenoGel (Loading) at all time points; TenoGel (tECM) showed significantly higher tenogenesis ssGSEA score compared to TenoGel (Loading) at day 21; TenoGel (Loading) showed significantly higher ssGSEA osteogenesis scores compared to TenoGel (tECM+Loading) and TenoGel (tECM) at day 21 (Figure 3E). Next, in vitro pre-conditioning duration was evaluated by performing gene set enrichment analysis (GSEA) for "tenocyte" gene sets from the TISSUE database.[54] The results showed that hASCs cultured in the TenoGel (tECM+Loading) at day 10 had enhanced expression of tendon-related genes (higher normalized enrichment score; NES) compared to day 6 and day 21, whereas TenoGel (tECM+Loading) at day 21 exhibited enriched senescence-related gene sets (Figure 3F,G). This suggested that a-10 day pre-conditioning period was sufficient to achieve the desired tendon phenotype, and overly long durations (day 21) were subpar.

We further explored the signalling mechanisms involved in hASCs' response to tECM and tensile loading within TenoGel (**Figure 4**A). Gene Ontology (GO) analysis revealed that tECM in TenoGel primarily contributed to "collagen fibril organization" and the "transmembrane receptor protein tyrosine kinase signaling pathway", while loading was associated with the "integrin-mediated signaling pathway" and "cell adhesion" in hASCs (Figure S3, Supporting Information). Further refinement using REVIGO highlighted "ECM organization" and "skeleton system development" as the most significant events in TenoGel (tECM+Loading) with 10-day pre-conditioning, characterized by increased expression of collagens and tendon matrix proteins (e.g., *COL1A1, COL3A1, ELN, COMP*, and *THBS1*) compared to Gel (Ctrl) (Figure 4B). Compared to Gel (Ctrl), TenoGel (tECM), TenoGel (Loading), and TenoGel (tECM+Loading) all showed the activation of key pathways such as "protein digestion and absorption", "ECM receptor interactions", "focal adhesion", and "PI3K/Akt" at all time points (Figure 4C). Specifically, the enrichment of "protein digestion and absorption" was associated

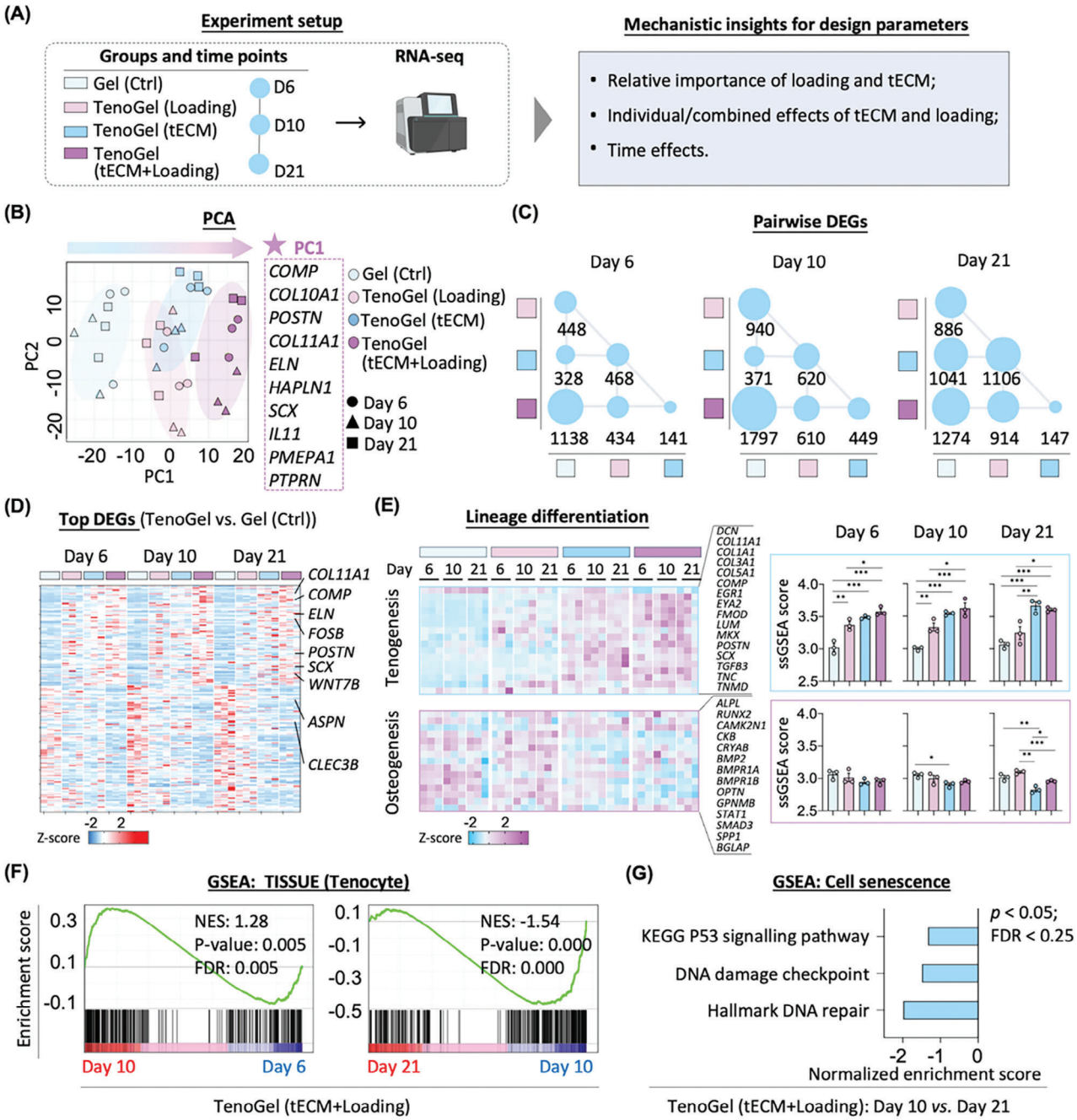

Figure 3. Transcriptional analysis of hASC lineage differentiation in response to different TenoGel designs. A) Study overview: the schematic illustrates the experimental setup and TenoGel design considerations. $n = 3$ biological replicates. B) PCA: The PCA plot and the presentation of the top 10 genes demonstrated that the divergence in transcriptional profiles among different TenoGel groups was primarily driven by tendon-related markers. C) DEGs: the pairwise comparison of transcriptional profiles across different TenoGel designs revealed that the largest numbers of DEGs were observed between TenoGel (tECM+Loading) and the Gel (Ctrl) group. The size of the circles represented the number of DEGs, as indicated in the legend. D) Top DEGs: the DEG heatmap displayed the top 20 upregulated and top 20 downregulated DEGs in the comparison of TenoGel (Loading)/(tECM)/(tECM+Loading) versus Gel (Ctrl) at respective time point, along with their representative marker genes. E) Lineage differentiation: the heatmap and quantitative analysis (ssGSEA) of genes associated with tendon and bone lineages suggested that TenoGel groups, with the tECM and w/o loading, exhibited enhanced tenogenesis over time. However, TenoGel (loading) also induced osteogenesis with the culturing. $n = 3$ biological replicates; mean ± SEM; *, $p < 0.05$; **, $p < 0.01$; ***, $p < 0.001$. F) GSEA (TISSUE (Tenocyte)): the enrichment plots revealed that pre-conditioning of TenoGel (tECM+Loading) for 10 days achieved a significantly higher NES associated with tendon-specific signature genes compared to pre-conditioning for 6- and 21- days. Presented NES are significant ($p < 0.05$, FDR < 0.25). G) GSEA (cell senescence-related pathways): Negative NES values indicate enrichment pre-conditioning of TenoGel (tECM+Loading) for 21 days induced the activation of cell senescence pathways compared to pre-conditioning for 10 days. Presented NES are significant ($p < 0.05$, FDR < 0.25).

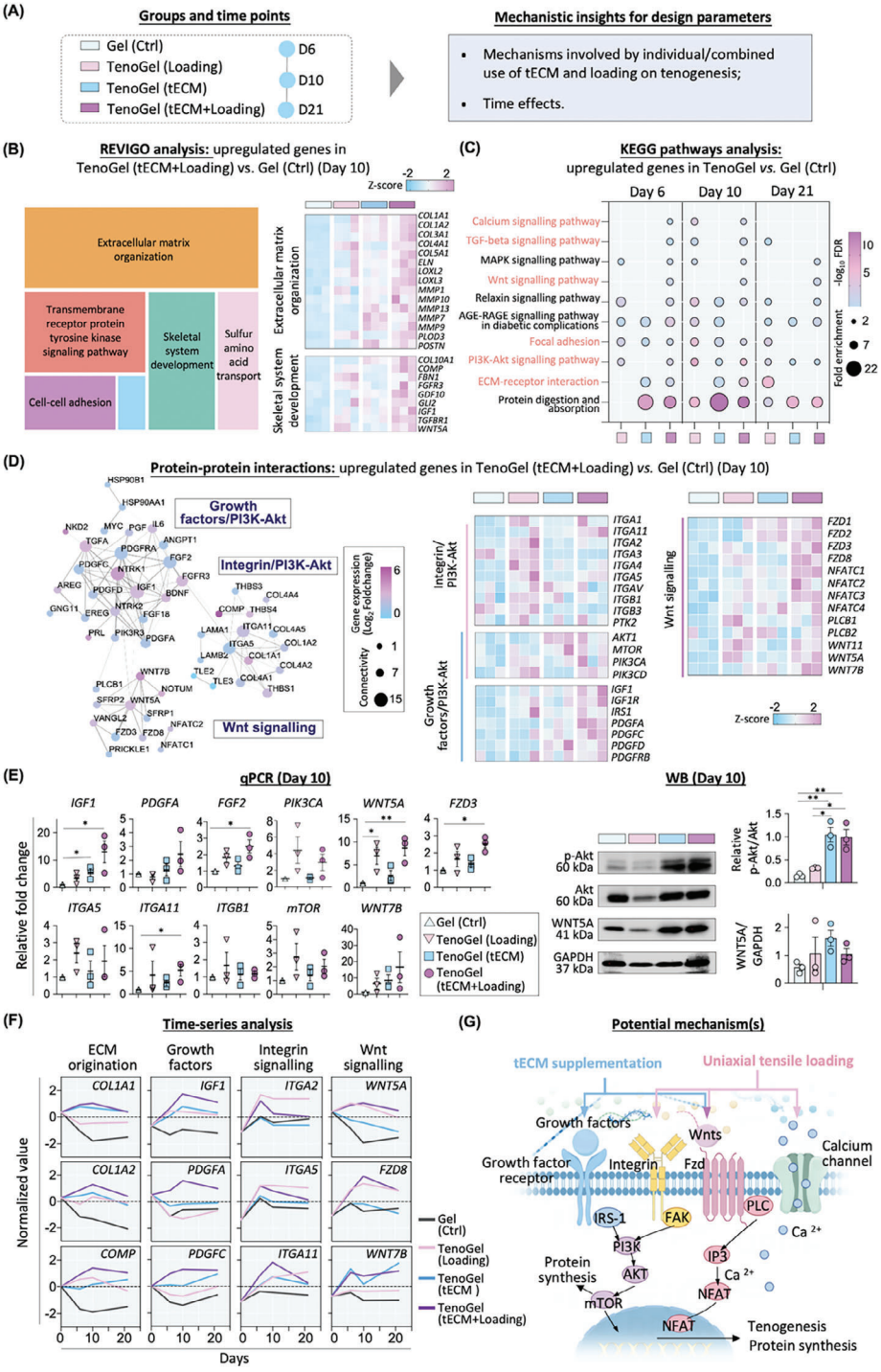

Figure 4. Transcriptional insights of induced signaling mechanisms in response to different TenoGel designs. A) Study overview: the schematic illustrates the experimental setup and TenoGel design considerations. B) REVIGO analysis clusters all identified GO terms of biological processes into broader categories among TenoGel (tECM+Loading) compared to Gel (Ctrl) at day 10. Additionally, the heatmap illustrated the expression levels of related genes associated with selected GO terms in hASCs. C) KEGG: the significantly enriched pathways were identified among different TenoGels (Loading)/(tECM)/(tECM+Loading) compared to the Gel (Ctrl) group on days 6, 10, and 21. D) PPI: A PPI network was constructed using upregulated genes associated with PI3K/Akt and Wnt signaling pathways. Additionally, the heatmap illustrated the expression levels of related genes in each TenoGel group and Gel (Ctrl) group at day 10. E) qPCR and WB analysis of hASCs cultured in different TenoGel groups on day 10. $n = 3$ biological replicates; mean ± SEM; *, $p < 0.05$; **, $p < 0.01$. F) Time-series analysis: the expression profiles of genes associated with key pathways in different TenoGel groups over time were presented. G) Potential mechanism: the schematic illustrated the potential involvement of growth factors/PI3K/Akt, integrin/PI3K/Akt, and Wnt signaling pathways in hASC tendon differentiation and related protein synthesis in response to different TenoGel designs.

with the upregulation of collagen-related genes. Within the PI3K-AKT pathway, TenoGel (Loading) showed upregulated expression of integrins (such as *ITGA2, ITGA4*, and *ITGA*5), while TenoGel (tECM) showed upregulated expression of growth factors (such as *PDGFD*) (Figure 4C; Figure S4, Supporting Information), suggesting that tECM and loading may activate the PI3K/Akt signaling pathway through distinct mechanisms. Notably, only TenoGel (tECM+Loading) specifically activated the "Wnt signaling pathway", with *WNT5A* predicted as a core gene that interacts with most of the other genes in the genes clusters (Figure 4D). Additionally, GSEA revealed significant enrichment of the PI3K/Akt and Wnt signaling pathways in TenoGel groups (i.e., TenoGel (tECM), TenoGel (Loading), and TenoGel (tECM+Loading)) compared to Gel (Ctrl) group at day 10 (Figure S5, Supporting Information). These findings are consistent with previous studies that have demonstrated the activation of the PI3K/Akt pathway by mechanical stimulation or ECM proteins for MSCs tenogenic differentiation.[55–57] Taken together, our results along with supporting evidence from the literature suggest that both tECM supplementation and mechanical loading, either independently or in combination, promote hASC tenogenesis within TenoGel, potentially via the activation of the PI3K-Akt and WNT pathways. To investigate the activation of the PI3K-Akt and Wnt pathways, we utilized qPCR and Western blot (WB) to examine the expression of core genes and proteins associated with these pathways (Figure 4E). After 10 days of in vitro pre-conditioning, qPCR analysis revealed that TenoGel (tECM) significantly upregulated the expression of *IGF1*, a core gene in the growth factor/PI3K-Akt signaling pathway, compared to the Gel (Ctrl) group. Although TenoGel (Loading) upregulated the *ITGA5*, the difference was not statistically significant. Notably, TenoGel (tECM+Loading) demonstrated significant upregulation of *IGF1*, *FGF2*, and *ITGA11*, which are core genes involved in the PI3K-Akt signaling pathway, compared to the Gel (Ctrl) group. For the Wnt signaling pathway, all TenoGel groups showed differential upregulation of markers compared to the Gel (Ctrl) group, with TenoGel (tECM+Loading) showing more pronounced upregulation of the *FZD8* and *WNT5A* genes. The WB and its semi-quantitative analysis showed that the p-Akt/Akt ratio in the TenoGel (tECM) and TenoGel (tECM+Loading) groups was significantly higher than that in the Gel (Ctrl) group. Additionally, all TenoGel groups exhibited higher WNT5A synthesis compared to the Gel (Ctrl) group, although the difference was not statistically significant. Collectively, these results suggest that the involvement of PI3K-Akt and Wnt signaling pathways induced by the tECM and mechanical loading in the TenoGel.

We also conducted a time series analysis focusing on key genes associated with ECM organization, integrin, growth factor/PI3K/Akt, and Wnt signaling pathways (Figure 4F). The analysis revealed distinct expression profiles in the TenoGel (tECM) and TenoGel (tECM+Loading) groups compared to the other two groups. Specifically, within the ECM organization pathway and growth factor/PI3K/Akt signaling pathway, there was an initial upregulation in the expression of genes associated with ECM organization (such as *COL1A1*, *COL1A2*, and *COMP*) and growth factors (such as *IGF1*, *PDGFA*, and *PDGFC*) until day 10, followed by subsequent declines. Additionally, genes involved in the integrin pathway and Wnt signaling pathway, including integrin subunits, *WNT5A*, and the Wnt protein receptor *FZD8*, consistently demonstrated higher expression levels and displayed an additional peak at day 10 in the TenoGel (Loading) and TenoGel (tECM+Loading) groups, where as such patterns were not observed in the other two groups.

Therefore, the bioinformatics analysis provides the following critical insights for designing the optimal TenoGel: (1) Synergistic effects: the combination of tECM and tensile loading within the TenoGel synergistically promotes robust tendon differentiation (Figure 4G). (2) Pre-conditioning duration: a 10-day pre-conditioning period is sufficient to achieve the desired tendon phenotype, while overly long durations (day 21) result in reduced tenogenesis and increased senescence. (3) Relative significance: tECM plays an essential role in inducing hASC tendon differentiation, whereas tensile loading alone is not specific to the tendon lineage and could potentially shift hASCs toward osteogenesis without tECM supplementation. In summary, the optimal TenoGel design should incorporate the synergistic combination of tECM and tensile loading, along with a 10-day pre-conditioning period, to achieve robust tenogenesis and prevent undesired osteogenic differentiation.

2.4. Mathematical Models for the Evaluation and Prediction of the Effects of TenoGel Design on hASC Tenogenesis and Osteogenesis

Using transcriptomes generated from Gel (Ctrl), TenoGel (Loading), TenoGel (tECM), and TenoGel (tECM+Loading) groups at days 6, 10, and 21, mathematical models were applied to quantitatively assess and predict the impact of TenoGel designs, i.e., individual and combined use of tECM and tensile loading, on hASC tenogenic and osteogenic differentiation (**Figure 5**A).

The initial step was to generate an overall scoring system to assess tenogenic and osteogenic lineage commitment of hASCs, which was based on 81 canonical lineage-specific marker genes (Figure 5B; and Table S1, Supporting Information). Subsequently, we fitted the tenogenic and osteogenic scoring data from 36 samples of four different groups using random forest (RF, 500 trees (Figure S6, Supporting Information)) and linear regression (LR) models (Figure 5C). To assess model performance fairly, 3-fold cross-validation (CV) was used to train and evaluate each model on each lineage independently. Specifically, the dataset was randomly split into three disjoint sets, and each set was used as the validation set once while the remaining two sets were used as the training set. Overall, both RF and LR models demonstrated good model fits for hASC tenogenic differentiation in TenoGel, as evidenced by R-squared (R^2) values of 0.58 for RF and 0.64 for LR in the validation sets. For predicting tenogenic differentiation, the LR model outperformed RF with a lower validation mean squared error (*MSE*). However, both RF and LR models showed weak fit to osteogenic differentiation, with R^2 values of 0.28 for RF and 0.35 for LR. As further support, when predicted scores were plotted against observed differentiation scores, high association was noted in the validation sets for all 3-splits for tenogenic prediction (averaged *Pearson's* $r = 0.8$ for both RF and LR), but there was low-to-medium association observed for osteogenic prediction (averaged *Pearson's* $r = 0.58$ for RF and 0.6 for LR) (Figure 5C; Figure S7, Supporting Information).

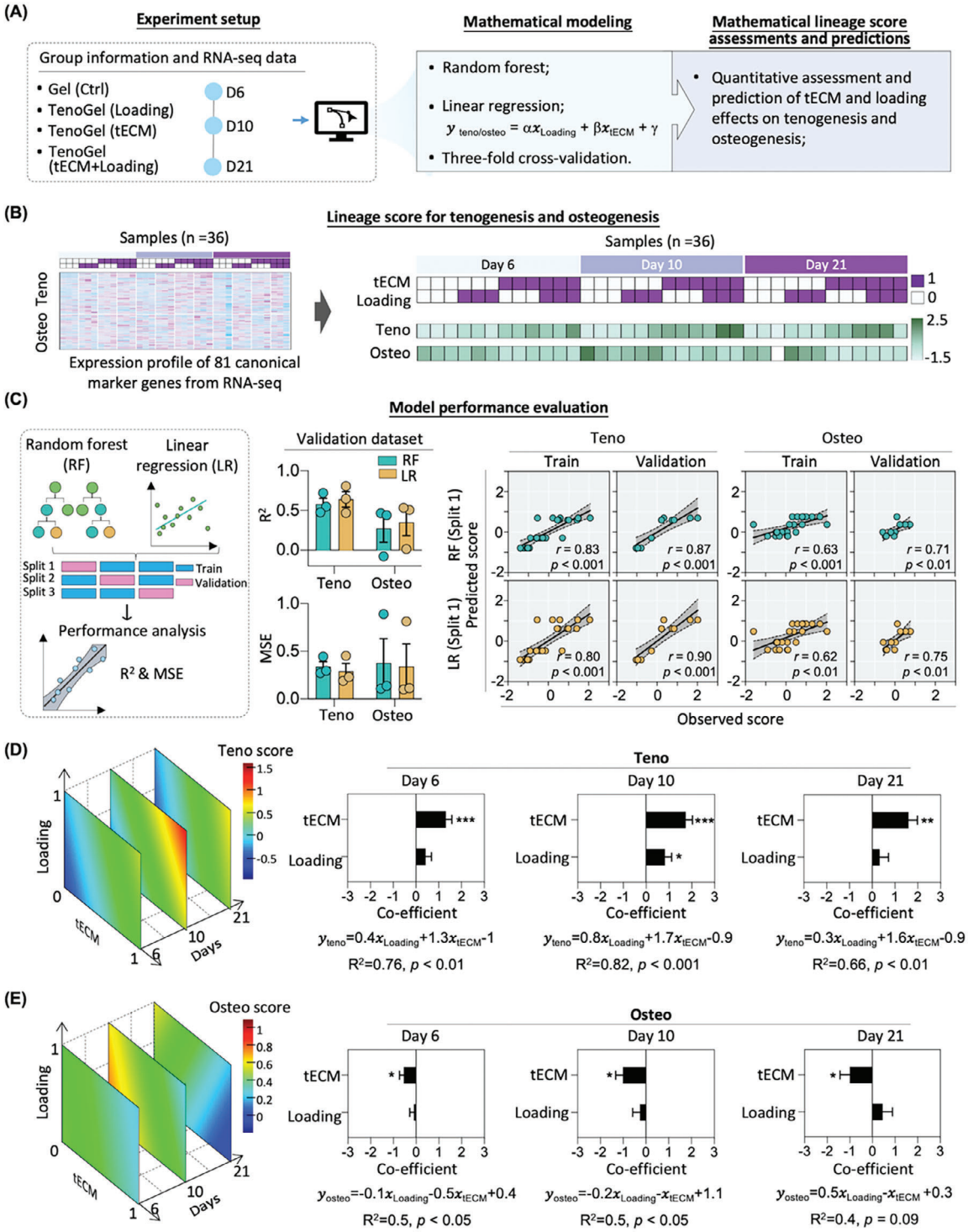

Figure 5. Mathematical modeling and evaluations of the effects of TenoGel design parameters on hASC transcriptome. A) Study overview: the schematic illustrates the experimental setup and key design considerations. B) Lineage scoring for assessing hASC tenogenic and osteogenic differentiation: A total of 81 genes associated with stem cell tenogenic (teno) and osteogenic (osteo) differentiation were selected based on the literature. The Heatmap visualization of teno/osteo scores, derived from the transcriptomic data of hASCs in each TenoGel group, was presented. C) Model performance evaluation: The R^2 and MSE of the testing datasets were used to evaluate the performance of the RF and LR models. The evaluation was conducted using three-fold cross-validation based on the training and validation datasets. The scatter plots showed the predicted and observed differentiation scores from the first split of each model. mean ± SEM. D,E) LR models: 4D regression plot and multiple LR models were established to compare the effects of relative importance of TenoGel parameters on hASC tenogenic and osteogenic differentiation over time (panel D: teno score; panel E: osteo score). mean ± SD; *, $p < 0.05$; **, $p < 0.01$; ***, $p < 0.001$.

To assess the individual contributions of tECM, loading, and in vitro pre-conditioning duration in TenoGel in hASC tenogenesis and osteogenesis, we constructed multiple LR models using all 36 samples, with tECM and loading as predictors, and the tenogenic/osteogenic scores as the outcomes at each time point, respectively. The LR model demonstrated that both tECM supplementation and uniaxial tensile loading were significantly associated with tenogenic scores (R^2 = 0.66–0.82, $p < 0.001$), with a more pronounced effect at day 10. Specifically, the estimated equation at day 10, $y_{teno} = 0.8x_{Loading} + 1.7x_{tECM} - 0.9$, indicated that tECM had a stronger effect, with the addition of 1.5 mg mL^{-1} tECM supplementation in TenoGel resulting in an ≈1.7 unit increase in the tenogenic score when loading was held constant ($p < 0.001$) (Figure 5D). Similarly, applying loading resulted in an ≈0.8 unit increase in the tenogenic score when tECM was held constant ($p < 0.01$). In terms of predicting osteogenic differentiation of hASCs in response to TenoGel features, the weaker fit of the LR model for osteogenesis (R^2 = 0.4–0.5) suggested a lower association (Figure 5E). It was estimated that applying loading did not result in a significant change in the osteogenic score when tECM was held constant. On the contrary, the addition of supplementary tECM led to a decrease in the osteogenic score by ≈1 unit when loading was held constant at day 10 ($p < 0.001$). We also fit LR models to investigate the impact of in vitro pre-conditioning duration (days 6, 10, and 21) on hASC tenogenic and osteogenic differentiation in various TenoGel groups. Both models showed a positive and strong association between time points and differentiation scores for tenogenic and osteogenic differentiation ($p < 0.01$, R^2 = 0.67 and 0.96). Notably, for tenogenic scores, day 10 had a larger effecter size, as indicated by its higher coefficient of 2.63 ($p < 0.01$) (Table S2, Supporting Information).

Thus, regarding the optimal design of TenoGel, the mathematical models provided the following recommendations: (1) tECM had a greater impact on tenogenic scores compared to the loading stimulation and hinted at a negative correlation with osteogenic scores. This suggests the tECM is a must-have component in the TenoGel design. (2) tECM should be used at the highest soluble concentration of 1.5 mg mL^{-1}, as there is a positive linear correlation between tECM concentration and tenogenic differentiation. (3) The tECM should be used in combination with tensile loading within TenoGel, along with a 10-day pre-conditioning duration. This is because the regression models showed positive correlations between both tECM and loading with tenogenic scores, with the most significant impact observed on day 10. These findings from the machine learning-based modeling align with the results obtained from the RNA-seq bioinformatics analysis, leading to a consistent conclusion regarding the optimal design parameters for TenoGel.

2.5. TenoGel with tECM and Uniaxial Tensile Loading Synergistically Promoted hASC Tenogenesis In Vitro

To showcase and validate the benefits of using our in-house transcriptome data (RNA-seq analysis and mathematical modelling) for TenoGel design optimization, we have performed in further in vitro and in silico analyses.

Building upon the insights generated from bioinformatics analysis (Figures 3 and 4) and mathematical modelling (Figure 5), the TenoGel (tECM+Loading) exhibited the most promising tenogenic potential. Therefore, we first evaluated the synergistic effects of tECM and tensile loading within TenoGel in promoting hASC tendon differentiation using qPCR and immunofluorescence (IF) analyses of established tenogenic markers (**Figure 6A,B**). After 10 days of culture, qPCR confirmed upregulation of established tenogenic markers in the TenoGel (tECM+Loading) group compared to Gel (Ctrl) group, with significantly increased expression of *SCX* (62.6-fold, $p < 0.01$) and *COL1A1* (8.6-fold, $p < 0.05$). Consistently, IF staining results revealed that TenoGel (Loading), TenoGel (tECM), and TenoGel (tECM+Loading) had increased protein abundance of TNC compared to Gel (Ctrl) on days 6, 10, and 21. Notably, TenoGel (tECM+Loading) exhibited more pronounced staining for TNMD, a late tendon differentiation marker,[58] compared to the other groups at day 21 (Figure 6B). Collectively, these findings suggest that both tECM supplementation and mechanical loading can promote hASC tenogenic differentiation in TenoGel, with their combination showing a strong synergistic effect.

Furthermore, bioinformatic analysis and mathematical modelling indicated that tECM is crucial for inducing hASC tendon differentiation, whereas tensile loading alone could shift hASCs toward osteogenesis without tECM supplementation. To evaluate this finding, we cultured hASCs in TenoGel with osteogenic medium and assessed hASC mineralization using Alizarin Red S (ARS) staining (Figure 6C). After 21 days, all groups showed different levels of mineral deposition. The TenoGel (Loading) group exhibited the highest mineral accumulation compared to all other groups, including TenoGel (tECM) and TenoGel (tECM+Loading) groups. These findings suggest that loading alone can lead to enhanced hASC mineralization, while tECM did not show strong mineralization effects, whether used alone or in combination with loading, consistent with the RNA-seq results (Figure 6C).

The bioinformatic analysis and mathematical modeling suggested that a longer in vitro pre-conditioning duration, i.e., 21 days, can induce cell senescence and may not be ideal for TenoGel design. To further support this, we compared senescence-associated beta-galactosidase (SA-β-gal) activity in hASCs after 6, 10, and 21 days of pre-conditioning within TenoGel (tECM+Loading) (Figure 6D). SA-β-gal staining revealed a significant increase in the ratio of senescent cells over time, with the highest percentage (≈41%) observed on day 21 (Figure 6D). These findings indicate that a longer in vitro pre-conditioning duration can induce pronounced cell senescence.

Furthermore, we set up additional TenoGel design groups (i.e., tECM with reduced concentrations with or without loading), and further tested the predictive accuracy of our mathematical models (Figure S8A, Supporting Information). Heatmap and ssGSEA showed significantly higher tenogenesis score in TenoGel groups (half tECM+Loading) compared to Gel (Ctrl) and TenoGel (half tECM) groups (Figure S8B, Supporting Information). Additionally, heatmap analysis of osteogenic marker genes showed decreased osteogenic differentiation in TenoGel (half tECM) and TenoGel (half tECM+Loading) groups, although there was no significant difference evaluated by ssGSEA score of osteogenesis (Figure S8B, Supporting Information). We then used transcriptomics data from TenoGel (half tECM) and TenoGel (half tECM+Loading) under unseen conditions to validate the predic-

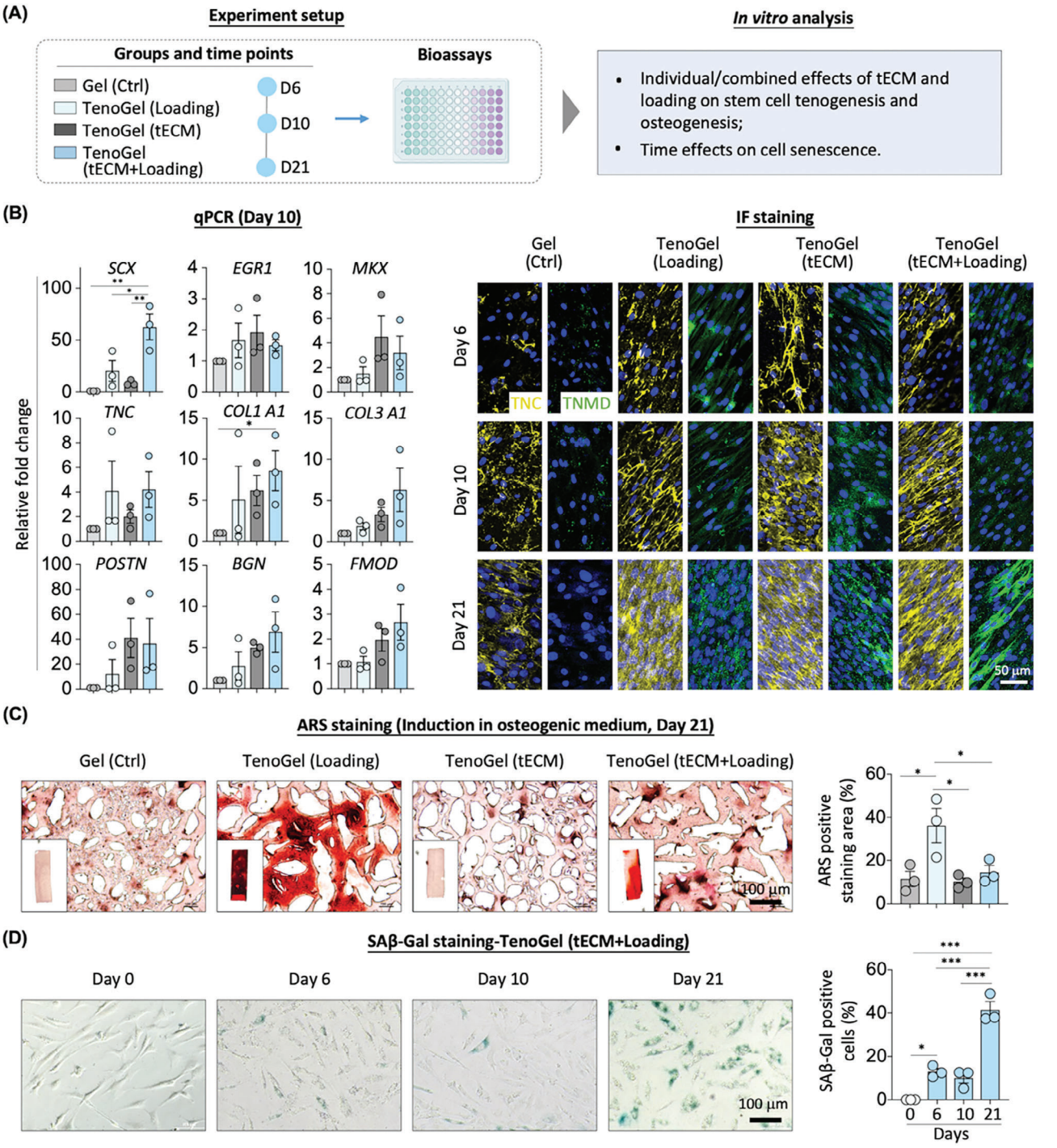

Figure 6. In vitro analysis of optimized TenoGel design. A) Study overview: schematic illustrated the experimental setup and in vitro validation. $n = 3$ biological replicates. B) qPCR: the expression levels of established tendon marker genes in hASCs cultured under different TenoGel groups on day 10 are presented. mean ± SEM; *, $p < 0.05$; **, $p < 0.01$. IF staining: representative confocal images are shown, depicting the staining intensity of TNC and TNMD in hASCs cultured in different TenoGel groups on days 6, 10, and 21 (yellow, TNC; green, TNMD; blue, nuclei). These results demonstrated that the presence of tECM supplementation and stimulation of uniaxial tensile loading in TenoGel synergistically promoted hASC tenogenic differentiation. C) ARS staining and semi-quantitative analysis: Representative histologic sections of hASCs cultured in various TenoGel groups with osteogenic medium on day 21. The red color indicates positively stained areas of calcium nodes, reflecting mineral accumulation. These findings suggest that loading alone can lead to enhanced hASC mineralization, while tECM did not show strong mineralization effects, whether used alone or in combination with loading. mean ± SEM; *, $p < 0.05$. D) SAβ-Gal staining and semi-quantitative analysis: Representative microscopic images of hASCs in TenoGel (tECM+Loading) after 6, 10, and 21 days of pre-conditioning. Cells stained with blue indicate positive staining for SAβ-Gal. These findings indicate that longer in vitro pre-conditioning duration induces more pronounced cell senescence. mean ± SEM; *, $p < 0.05$. ***, $p < 0.001$.

tive performance of our models. The models demonstrated good generalizability for predicting tenogenic scores, with an MSE of 0.24 on these external test sets, which was lower than the MSE obtained from the internal CV set. However, the models performed poorly in predicting osteogenic scores, indicated by a relatively high MSE of 0.79 (Figure S8C, Supporting Information). These findings validate the predictive accuracy of our established model for hASCs tenogenesis using the parameters from TenoGel.

In conclusion, our findings further showcase the benefits of using our in-house transcriptome data for TenoGel design optimization. Key insights include that tECM and loading should both be used in TenoGel design to achieve the positive combined effects of promoting hASC tenogenesis. Also, tECM supplementation in TenoGel is a critical factor, as tensile loading alone without tECM showed enhanced hASC mineralization, indicating a shift toward osteogenesis. Furthermore, our results suggest that an in vitro pre-conditioning duration of 10 days is better than 21 days, as the longer duration can lead to an undesirable increase in stem cell senescence. Finally, our mathematical models exhibited the generalizability of the predictive models for hASCs tenogenesis.

2.6. TenoGel Promoted Stem Cell Viability and Retention, as well as Enhanced Tendon Regeneration in a Rat Tendon Defect Model

As described earlier, TenoGel (tECM+Loading) with 10 days preconditioning duration demonstrated the most robust tenogenesis based on transcriptomic analysis and mathematic models (Figures 4 and 5). To evaluate the tendon healing effects of the in vitro preconditioned ASC-TenoGel, we further utilized a rat patellar tendon injury model (**Figure 7A**). This animal model can mimic clinical scenarios of tendon injuries, such as iatrogenic injuries that occur during anterior cruciate ligament reconstruction surgery.[59] Importantly, this model also serves as a well-established platform for studying ectopic ossification, which can occur during tendon healing and pathogenesis.[5] Therefore, this animal model provides an effective assessment of whether our TenoGel can promote robust tendon regeneration and prevent undesired ossification in stem cell-mediated tendon therapy. The experimental groups included (1) "Defect only": the tendon defects were created without hydrogel implantation; (2) "Gel only": cell-free GelMA/OA hydrogels were implanted onto the tendon defects; (3) "rASCs-Gel (Ctrl)": rat adipose-derived stem cells (rASCs) seeded in GelMA/OA hydrogel in static culture for 10 days before implanted onto the tendon defects; and (4) "rASCs-TenoGel (tECM+Loading)": rASCs seeded in TenoGel (tECM+Loading) for 10 days before implantation onto the tendon defects. Uninjured tendons on the contralateral side of the animals were designated as the intact control (intact ctrl) for comparative analysis. The viability of rASCs and tendon healing were assessed at designated time points.

The retention and survival of transplanted cells at the injury site are crucial for cell-based tendon therapy, as this ensures the continuous release of bioactive factors for regeneration.[60] The mechanical properties of the cell-hydrogel constructs derived from rASCs-Gel (Ctrl) and rASCs-TenoGel (tECM+Loading) were comparable after 10 days pre-conditioning as determined by tensile loading tests (Figure S9A, Supporting Information). To evaluate the viability of implanted rASCs, the fluorescence intensity of DiR-labeled rASCs was monitored at multiple time points, including day 0 before implantation, as well as at day 1 and week 1, 2, 4, 6, and 8 after implantation. As a negative control group, cell-free hydrogels showed minimal fluorescence signal (Figure S9B, Supporting Information). On day 1 postimplantation, fluorescence signals were observed in the grafted areas of both rASCs-Gel (Ctrl) and rASCs-TenoGel (tECM+Loading) groups. Importantly, the DiR-positive signals remained detectable in both the rASCs-Gel (Ctrl) and rASCs-TenoGel (tECM+Loading) at 4-weeks postimplantation (≈50% of day 1) and 8-weeks postimplantation (≈15% of day 1), indicating sustained retention and viability of the transplanted cells (Figure 7B). These findings suggest that the GelMA/OA hydrogel was capable of supporting the long-term retention and viability of rASCs in vivo.

Subsequently, we evaluated patellar tendon gross morphology, as aberrant tendon size has been reported to cause functional deficits following injuries, and vice versa.[61] At 8-weeks postimplantation, no obvious tendon defects were observed in the rASCs-TenoGel (tECM+Loading) group, while a clear defect remained in all other injured groups. The rASCs-TenoGel (tECM+Loading) group exhibited comparable length and cross sectional area (CSA) as the intact control tendons, whereas the other injured groups displayed longer tendon length and larger CSA (Figure 7C). Additionally, since the restoration of mechanical properties is crucial for the proper tendon functionality, tensile testing was performed on regenerated tendons at 8-weeks postimplantation. Failure mode analysis revealed that the intact control tendons primarily experienced ruptures at the patellar tendon-tibial bone junction. Similarly, the rASCs-TenoGel (tECM+Loading) group exhibited a 40% failure rate at the patellar tendon-tibial bone junction, whereas all other injured groups demonstrated a strong tendency (100%) for ruptures at the patella tendon-tibial bone junctions (Figure 7D). Moreover, the rASCs-TenoGel (tECM+Loading), not the other groups, achieved comparable stiffness (50.9 ± 3.6 N mm^{-1}), failure load (95.3 ± 4.8 N), and tensile modulus (58.8 ± 17.3 MPa) as intact tendons. Although the rASCs-TenoGel (tECM+Loading) group exhibited increased failure stress compared to the other injured groups, this value was still lower than intact control tendons (Figure 7D). Collectively, our results demonstrated that the rASCs-TenoGel (tECM+Loading) group effectively restored the tensile properties of the injured tendons, as an important indicator of tendon functional recovery.[62]

Tendon healing was compared histologically among different groups at 4- and 8-weeks postimplantation. At 4-weeks postimplantation, the rASC-TenoGel (tECM+Loading) group showed similar histological features as the intact control group (**Figure 8A**). Specifically, hematoxylin and eosin (H&E) staining and semi-quantitative analysis of cell alignment showed that rASCs-TenoGel (tECM+Loading) exhibited spindle-shaped cells and aligned, wavy ECM structure, whereas the Defect only, Gel only and rASCs-Gel (Ctrl) groups displayed rounded cells and disorganized ECM structure (Figure 8A). Moreover, Picrosirius Red (PSR) staining examined with polarized light microscopy as well as associated semi-quantitative analysis revealed increased birefringence and thicker (red-orange) collagen fibers in the rASC-treated groups, i.e., rASCs-Gel (Ctrl) and rASCs-TenoGel (tECM+Loading), compared to the Defect only and Gel only

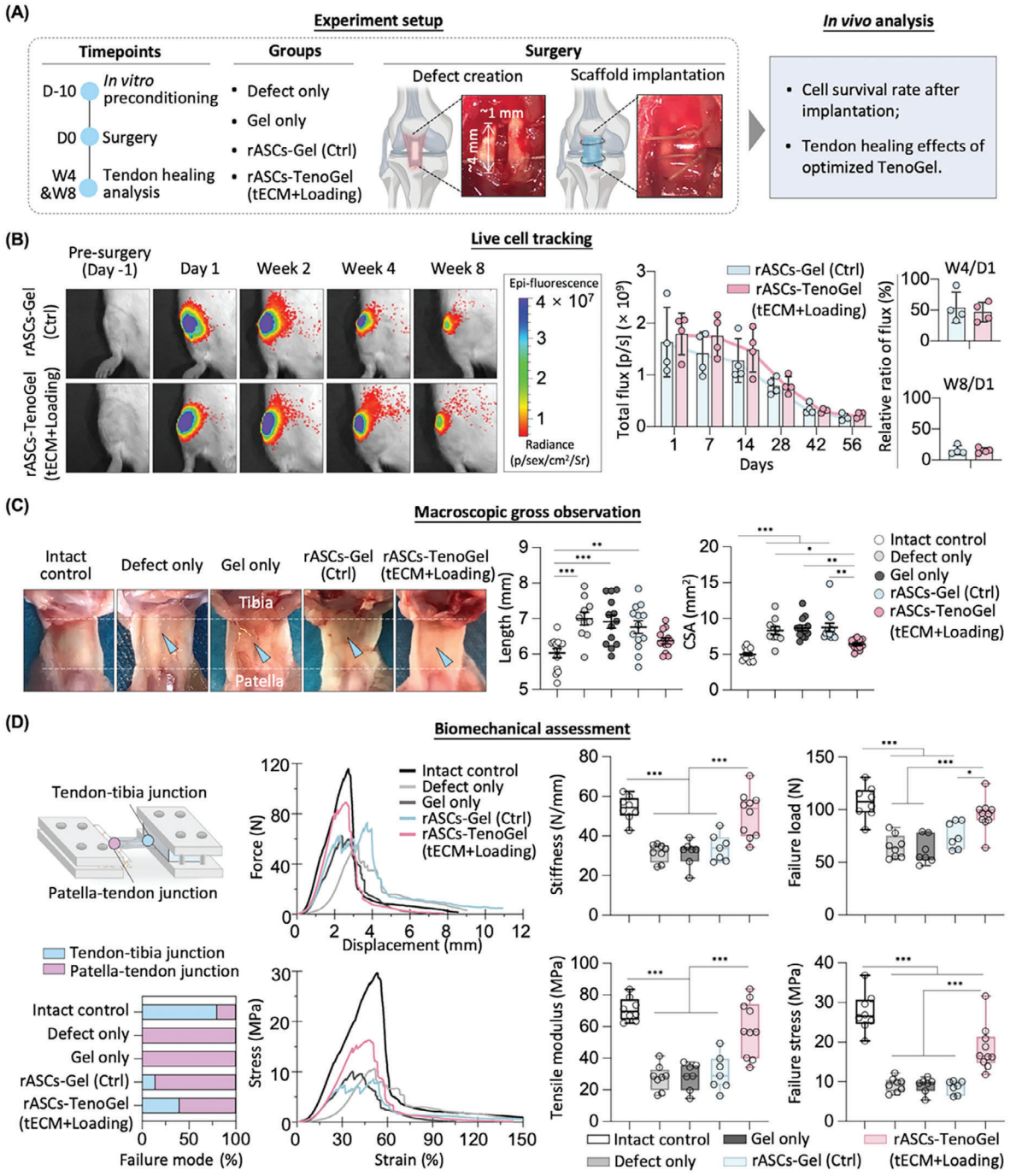

Figure 7. Characterization of optimized TenoGel with rASCs for tendon repair in a rat tendon defect model. A) Study overview: schematic showing the experimental setup. The experimental groups included: 1) "Defect only": the tendon defects were created without hydrogel implantation; 2) "Gel only": cell-free GelMA/OA hydrogels were implanted onto the tendon defects; 3) "rASCs-Gel (Ctrl)": rASCs seeded in GelMA/OA hydrogel in static culture for 10 days and implanted onto the tendon defects; and 4) "rASCs-TenoGel (tECM+Loading)": rASCs seeded in tECM containing-GelMA/OA hydrogel in uniaxial tensile loading culture for 10 days and implanted onto the tendon defects. The uninjured tendons on the contralateral side were designated as the intact control (intact ctrl) for comparative analysis. B) Cell tracing: biodistribution and semi-quantitative analysis of DiR-labeled rASCs at designed time points after transplantation revealed that both the Gel (Ctrl) and TenoGel (tECM+Loading) supported the long-term retention and viability of rASCs post-implantation. $n = 4$ rats per group. C) Macroscopic observation: digital images and measurements of the length and CSA for repaired tendons at 8 weeks post-surgery are presented (blue arrow, defect site). n⩾10 rats per group; mean ± SEM; *, $p < 0.05$; **, $p < 0.01$; ***, $p < 0.001$. D) Biomechanical assessment: Representative load-displacement curves and mechanical parameters of tendons from different groups at 8 weeks post-surgery are presented. n⩾7 rats per group; min. to max.; *, $p < 0.05$; ***, $p < 0.001$. These results suggested that TenoGel (tECM+Loading) promoted rASCs-mediated tendon repair, as evidenced by improvements in macroscopic appearance and enhanced mechanical properties in a rat tendon defect model.

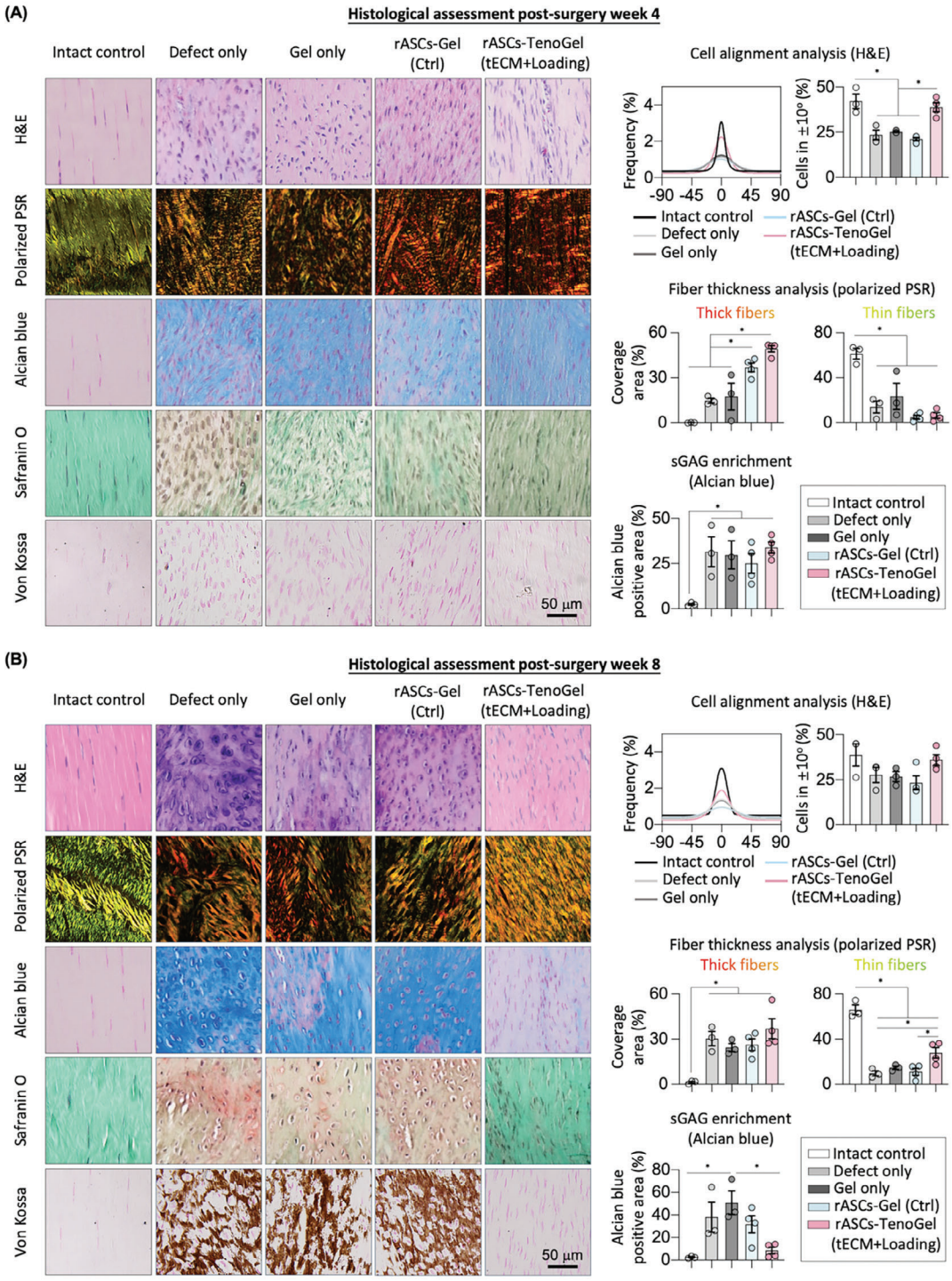

Figure 8. Histological evaluation of preconditioned, rASCs-TenoGel (tECM+Loading) for tendon repair in rat patellar tendon defect model. A,B) Histological assessment: representative histological images (H&E, Picrosirius Red (PSR), Alcian blue, Safranin O and Von Kossa staining) and semi-quantification analyses of tendons from different groups at week 4 and week 8 are presented. The rASCs-TenoGel (tECM+Loading) group exhibited improved cellular alignment compared to other injured groups at both 4 and 8 weeks, as observed in H&E staining. Additionally, polarized PSR indicated that the rASCs-TenoGel group exhibited more pronounced birefringence than the other injured groups, with a higher amount of orange-to-red (thicker) fibers at both 4 and 8 weeks. Furthermore, Alcian blue, Safranin O, and Von Kossa staining revealed the rASCs-TenoGel (tECM+Loading) group exhibited less sGAG and calcium deposition compared to the other injured groups at 8 weeks, similar to the intact tendon tissues. n⩾3 rats per group; mean ± SEM; *, $p < 0.05$. Overall, the histological analyses revealed that preconditioned rASCs-TenoGel (tECM+Loading) facilitated robust tendon healing at 8 weeks post-surgery compared to the other injured groups.

groups (Figure 8A). Alcian blue staining and its associated semi-quantitative analysis as well as Safranin O staining indicated the accumulation of sulfated glycosaminoglycan (sGAG) at 4-weeks in all injury groups (Figure 8A). At 8-weeks postimplantation, the rASC-TenoGel (tECM+Loading) group showed similar histological features as the intact control group (Figure 8B). Specifically, H&E staining and associated semi-quantitative analysis showed that that rASCs-TenoGel (tECM+Loading) exhibited a more compact and orderly aligned ECM reminiscent of native tendon, whereas the Defect only, Gel only and rASCs-Gel (Ctrl) groups all displayed degenerative features indicative of ectopic calcification (Figure 8B). The latter was evidenced by the emergence of a spontaneous ectopic calcified tissue surrounded by hypertrophic chondrocyte-like cells embedded within an sGAG/calcium-enriched matrix as evidenced by Alcian blue, Safranin O and Von Kossa staining (Figure 8B). Collectively, our results showed that the rASCs-TenoGel (tECM+Loading) group enhanced tendon repair, as evidenced by the restoration of a wavy, aligned collagen structure and the absence of ectopic ossification.

In summary, our animal model data collectively suggested that the delivery of rASCs in a mechanically robust and biocompatible GelMA/OA resulted in enhanced retention and viability of implanted rASC similar to our hypothesis. However, it is important to note that only rASCs pre-differentiated in a tendon-mimetic TenoGel with tECM and uniaxial tensile loading supplementation demonstrated the ability to promote functional tendon regeneration and avoid undesired ectopic calcification.

3. Discussion

This study presents a novel materiomics approach to guide the design of TenoGel for stem cell-mediated tendon repair – a significant advancement in the tendon research field. Unlike traditional empirical optimization, our materiomics strategy systematically explores the complex interplay between the TenoGel niche features and tenogenic differentiation using a transcriptome data-driven approach. The key highlights of this work are - (1) Integrated bioinformatics and mathematical modelling: we combined bioinformatics analysis with mathematical modelling based on RNA-seq data to provide in-depth mechanistic insights and quantitative assessment of optimal TenoGel design parameters; (2) Optimal TenoGel niche parameters: our findings addressed key design considerations for TenoGel to achieve robust tenogenesis, such as determining the relative importance of tECM and uniaxial tensile loading, the optimal tECM concentration, and in vitro pre-conditioning duration; (3) Strong validation in animal model: The optimized TenoGel (tECM + Loading) with preconditioned rat ASCs (10 days in vitro) exhibited enhanced tendon regeneration and avoided undesired bone formation in a rat tendon injury model. This strong correlation between the materiomics-guided TenoGel design insights and the in vivo tendon healing outcomes also underscores the potential of this data-driven strategy for biomaterial engineering solutions.

Although there are many hydrogel features that can potentially influence stem cell behavior, within our current study, we have chosen to focus on three key aspects in designing a tendon-mimetic hydrogel (TenoGel) niche. These features include a base material system comprised of an IPN-structured GelMA/OA hydrogel which could be further augmented by supplementation of tECM, and application of uniaxial tensile loading. The combination of these unique niche features within a 3D culture system is distinct from previous research, including our own investigation of the interplay between stiffness, topography or mechanical loading with growth in 2D settings.[10,13,25] First, the IPN structure is a critical feature of TenoGel, as it exhibited adequate mechanical toughness and slow degradation, facilitating tendon's long-term regeneration process.[46,63,64] Indeed, the GelMA/OA hydrogel used in current study possesses excellent biocompatibility, robust mechanical properties, and slow degradation profiles, withstanding in vitro loading for up to 21 days without rupture as well as supporting the long-term viability and local retention of the implanted rASCs (Figures 1, 2, and 7B). The GelMA/OA hydrogel was reported in one study for bone repair,[46] while its specific use for tendon repair remains relatively unexplored. Additionally, it is worth noting that the reported tensile modulus for hydrogels used in tendon repair typically falls within the range of 10–175 kPa.[6,7,65–67] In comparison, the GelMA/OA hydrogel exhibits an enhanced modulus, ≈236 kPa. Therefore, this mechanically reinforced GelMA/OA hydrogel holds promising potential for stem cell-mediated tendon repair for various scenarios, including the treatment of tendon full ruptures (Figure S10, Supporting Information). Additionally, to establish a tendon-mimetic hydrogel niche, the combined use of tECM as a biochemical cue and uniaxial mechanical loading as a biomechanical cue was also implemented.[21] tECM extracted by urea is highly enriched in collagens, non-collagenous matrix, and tenogenic growth factor.[9,19] Its biochemical composition is unique when compared to traditional acid pepsin-extracted ECM, which digest or deactivates most noncollagenous ECM. tECM is also highly bioactive and can induce robust tendon-specific differentiation of stem cells, whereas single/combined growth factors or skin-derived ECM may not exhibit tendon-specific bioactivity.[19,47] When investigating osteogenic differentiation, our findings revealed that the tECM-supplemented medium exhibited the least amount of undesired differentiation in terms of Alkaline Phosphatase (ALP) and ARS stainings, in contrast to the effects observed with osteogenesis medium and bone ECM (bECM) supplemented medium (Figure S11A, Supporting Information). This indicates the tissue-specifical bioactivity of tECM in promoting tendon differentiation, which is similar to our published work demonstrating that cartilage ECM extracted by urea also showed region-specific and tissue-specific bioactivity.[18] Furthermore, acknowledging the significance of mechanical stimulation in tendon fate commitment,[68–70] we incorporated specific uniaxial tensile loading combinations (8% strain, 0.5 Hz frequency, 6 h per day) into TenoGel. Extensive research has demonstrated the positive influence of controlled loading (6–10% elongation, 0.5-1 Hz frequency) on tenogenic differentiation outcomes.[24,55,71] In vitro mechanical stimulation offers several advantages in scenarios of stem cell pre-conditioning before in vivo implantation. For instance, precise modulation of specific loading regimens, including strain, frequency, and duration, is essential for effectively inducing stem cell differentiation toward the tendon lineage, as improper loading strains can result in stem cell differentiation into alternative lineages, such as adipose and bone.[21] Moreover, the optimal in vitro pre-conditioning duration is also a vital factor, since prolonged and curtailed cultures are associated with phenotypic drift,[72] and inadequate priming,[73] respectively. Although

post-injury physiological training shows promise in tendon healing, studies have also indicated that relying solely on natural mechanical stimulation in vivo may be insufficient for promoting tenogenesis.[74,75] Additionally, patient-customized physiological loading/training protocols based on their tendon injury location, the specific tendon involved, or patients' physical conditions, will be needed to warrant the desired healing outcomes.[39,76,77] In contrast, in vitro mechanical loading provides a more controllable environment for the precise regulation of stem cell differentiation toward the tendon lineage.

Although the importance of tendon ECM and loading stimulation in promoting tenogenesis is widely acknowledged, there is still a significant gap in our understanding regarding their relative significance and the optimal combination of these parameters required to induce robust tenogenesis. Thus, our materiomics strategy first utilized RNA-seq analysis to mechanistically decouple the effects of biomaterial features (tECM supplementation, uniaxial tensile stretching, and in vitro pre-conditioning duration) on hASCs transcriptome. This approach is similar to previous studies where both bulk and single-cell RNA-seq were used to investigate the influence of biomaterial features on tenogenic differentiation, including 3D culture environments,[78] substrate mechanical stiffness,[79] and bioactive components.[80] Our current study specifically focused on investigating the interactions of tECM and uniaxial tensile loading in terms of tendon differentiation. The RNA-seq results suggest that tECM is a critical key tenogenic factor that works synergistically with tensile loading to promote tendon differentiation, while the effects of loading are not specific to tendons (Figure 3E). Similar findings have been observed in previous experiments, whereby prolonged exposure to biochemical signals (e.g., FGF-2) abrogates the divergent effects of mechanical signals (material stiffness) on cell differentiation into either bone or tendon.[13] Mechanistically, our analysis further revealed that mechanical loading and tECM mediated PI3K/Akt pathway activation, which contributed toward hASC tenogenesis and tendon-related protein synthesis. Specifically, uniaxial tensile loading enhanced integrin gene expression, promoting cell-matrix interactions and activating the PI3K/Akt pathway. Our findings are in agreement with previous studies, which demonstrated that mechanical stimulation during tendon development activates the PI3K/Akt pathway through integrin signaling.[68] This activation plays a crucial role in mediating collagen assembly and facilitating the expression of tendon-associated genes. In addition, the tECM extract used here contains growth factors such as FGF-2, IGFBP-3, TGF-β1, and TGF-β3.[18] These growth factors have the potential to activate the PI3K/Akt pathway, with IGF-1 playing a key role in this process. Previous in vivo studies have demonstrated the essential role of IGF-1 signaling in normal postnatal tendon growth, which regulates tendon cell proliferation and protein synthesis through the coordination and crosstalk of the PI3K/Akt and ERK1/2 pathways.[81] Furthermore, uniaxial tensile loading and tECM synergistically activated non-canonical Wnt signaling pathway with *WNT5A* predicted as a core gene. While the Wnt signaling pathway is typically recognized as a classical signaling pathway that promotes osteogenic differentiation, recent studies have also indicated its involvement in tendon formation during embryogenesis.[82,83] Indeed, in vitro studies have found that *Wnt4* and *Wnt5a* play significant roles in the dynamic loading-induced tenogenic differentiation.[12] As further support, another study indicated that increased tendon-specific ECM production and enhanced collagen protein cross-linking were associated with upregulation of *WNT5A*.[84] However, existing studies on the direct effect of Wnt signaling on tendon differentiation are limited, and further investigations are needed.[85]

In addition to mechanistically evaluating the effects of TenoGel design on ASC transcriptome, our materiomics strategy also involves applying mathematical models and machine learning to quantitatively assess the relationship between TenoGel features and predict the hASC tenogenic and osteogenic commitment. Indeed, machine learning has been employed in the process optimization of scaffold preparation (e.g., bioprinting, electrospun fibers).[86] However, there is still a lack of exploration in understanding the effects of biomaterial features in terms of tendon differentiation.[21,87] Moreover, quantifying critical properties of biomaterials, including cellular proliferation and differentiation, presents a significant challenge.[88] To bridge this gap, a recent study employed a set of statistically designed experiments to evaluate the impact of biomaterial features on human stem cell tenogenic differentiation.[89] Their findings revealed relationships between matrix modulus, integrin-binding concentration in biomaterial, and tendon-related genes (*SCX*, *COL1A1*, and *TNC*). However, traditional methods like qPCR have inherent limitations in accurately assessing stem cell tenogenesis, thus hindering the establishment of an accurate mathematical relationship between material parameters and cellular phenotypes.[37] To overcome these limitations, we selected 81 canonical marker genes associated with tenogenesis and osteogenesis based on literature reviews (Table S1, Supporting Information). We further fitted the tenogenic and osteogenic scoring data using RF and LR models to capture relationships between TenoGel design and the outcomes of hASC tenogenic/osteogenic differentiation. The results demonstrated good model fits of hASC tenogenic differentiation in TenoGel using both RF and LR models, as evidenced by R^2 values of 0.58 for RF and 0.64 for LR (Figure 5C). Furthermore, the LR models (e.g., $y_{teno} = 0.8x_{Loading}+1.7x_{tECM}-0.9$) indicated that both tECM supplementation and uniaxial tensile loading in the TenoGel significantly predicted tenogenic scores ($R^2 = 0.82$, $p < 0.001$), with tECM estimated to have a stronger impact on tenogenic score. Additionally, based on the promotion of a larger tenogenic effect size, a period of 10-days was identified to be the most suitable duration for in vitro pre-conditioning. It is also noteworthy that for accurate predictions, it is recommended that the feature parameters of the materials fall within the range of the training data, such as tECM concentration ranging from 0 to 1.5 mg mL^{-1}.

Generally, grafting stem cells for in vivo tendon repair presents two primary challenges: low graft survival rates and the risk of ectopic tissue formation. Our in vivo findings highlight the following important discoveries: (1) TenoGel-mediated delivery of rASCs achieved prolonged cell survival and retention (up to 2-months postimplantation) (Figure 7B). The sustained presence of stem cells at the target site is crucial for tendon repair, achieved through the mechanisms of engrafted donor cells replacing damaged cells and the paracrine effect of donor cell-secreted growth factors promoting the host tissue's self-regenerative capacity.[90] In contrast, collagen or fibrin-based hydrogels which are most often used in pre-clinical trials typically fail to

provide long-term support, leading to postimplantation failure.[91–93]; (2) There was a significant positive contribution of our optimized TenoGel design for inhibiting off-target tissue formation during tendon repair. The implantation of rASCs-TenoGel (tECM+Loading), but not rASCs-Gel (Ctrl), resulted in proper tendon tissue repair with aligned collagen fibers, without the formation of mineralized bone tissue or sGAG matrix in vivo (Figure 8). Additionally, the Gel (Ctrl) and TenoGel (Loading) groups with rASCs exhibited enhanced mineral accumulation compared to the TenoGel (tECM) and TenoGel (tECM+Loading) groups under in vitro osteogenic induction (Figure S11B, Supporting Information). Preventing undesired ossification is crucial because ectopic ossification can impair tendon function and cause pain.[94,95] Our results confirmed that properly repaired tendon tissue exhibited improved mechanical properties, such as strength and stiffness, which were absent in tissues affected by ectopic calcification. To further validate the functional achievements of optimized TenoGel for stem cell-mediated tendon repair, it is necessary to conduct additional assessments, such as gait analysis, in future investigations.[96] Overall, both previous works and our study together emphasize the importance of pre-differentiating stem cells towards tendon cells in the appropriate environment before transplantation.[97–99]

Our current study had several limitations that highlight the need for further research in specific directions. First, to study the relationship between material parameters and cell lineages, we employed two models, random forest and linear regression. Although these models offer advantages in capturing diverse relationships, assigning continuous parameter values would have been advantageous for a more comprehensive understanding and enhanced accuracy and reliability of the models.[100] This becomes particularly important when assessing intricate designs that involve incorporating multiple design parameters, as these parameters can significantly influence the robustness of the mathematical models. Such limitation also includes that our mathematical model did not explore the relationships among the sub-parameters of loading. Uniaxial tensile loading, known for influencing stem cell tenogenic differentiation, encompasses multiple sub-parameters like loading strain, frequency, and duration.[71,87,101] Future research endeavors may focus on developing more intricate models that comprehensively define these relationships, enabling accurate prediction of stem cell tenogenesis based on specific loading regimens. Second, our model exhibited lower accuracy in predicting TenoGel features on hASCs osteogenic fate. This discrepancy may be attributed to specific material properties considered in TenoGel design, such as tECM and loading, which were primarily aimed at promoting tenogenic differentiation. In future investigations, it is important to incorporate other material parameters known to influence the teno/osteogenic differentiation of stem cells, including matrix topography,[102,103] stiffness,[13,104] viscoelasticity,[105,106] and other biochemicals like growth factors and small biomolecules.[10,21,107] These features should be thoroughly explored by integrating high-throughput platforms and advanced computational tools with our developed materiomics strategy to create a targeted design approach for developing a more robust tendon niche-like biomaterial.[108] Finally, while stem cell tenogenesis is a key factor for the success of stem cell-mediated tendon repair as well as our study's focus, it is important to acknowledge that other factors such as cell fate post-implantation and host immune responses may also influence the therapeutic outcomes.[109] Therefore, it is essential to consider these additional mechanisms when evaluating the overall effectiveness of tendon repair strategies. Also, more thorough investigations are still needed to explore the link between the materiomics readouts and in vivo behaviors of the implanted ASCs, as well as tendon healing outcomes. This is especially important for groups that have been evaluated in vitro, such as the rASCs-TenoGel (tECM) construct, but have not yet been assessed using an in vivo animal model.

Conventional approaches in biomaterial development often involve intuitive tailoring of multiple parameters, which can lead to long research and development cycles and high costs. In our study, we developed an innovative RNA-seq-based materiomics strategy, which allowed us to investigate the relative significance and synergistic contributions of individual or combined hydrogel niche features in promoting tendon differentiation. By leveraging this approach, we generated comprehensive knowledge that effectively parameterizes and correlates the intricate interplay between biology and materials. As a result, a more informed and targeted approach has been developed to streamline the biomaterials research and development process. This methodology presents great potential as an assessment and predictive tool in addition to traditional approaches, to achieve predictable and highly efficient healing outcomes within and beyond the scope of tendon regeneration.

4. Experimental Section

TenoGel Development and Characterization: To establish a tendon-biomimetic hydrogel environment for stem cell tenogenic preconditioning, inspired by the natural tendon microenvironment, TenoGel was established consisting of three major components: having tough biomechanical and slow degradation features, incorporating urea-extracted tECM as tendon-specific biochemical cues, stimulated with dynamic uniaxial tensile loading as a biomechanical cue. To sustain the dynamic mechanical loading in vitro and support the long-term healing of injured tendons, a previously developed IPN-structured hydrogel was developed using gelatin methacryloyl combined with oxidized alginate with minor modifications (Experimental Section, Supporting Information).[46] Additionally, a bioinspired strategy of using the ECM's rich biocomplexity was utilized for tissue-specific regeneration via unique urea-based protocol for collecting soluble, DNA-free tECM extracts, which were further incorporated into the GelMA/OA hydrogel during gelation process.[9] To fabricate hydrogels supplemented with tECM, GelMA/OA pre-polymer was mixed with tECM at a final concentration of 1.5 mg mL^{-1} and followed by the gelation procedures (Experimental Section, Supporting Information).

To ensure consistency in tECM extraction among various batches, several assays, including dsDNA assay, hydroxyproline assay, sGAG assay, SDS-PAGE, and tenogenic and osteogenic bioactivity test were performed as previously reported (Experimental Section, Supporting Information).[19] To characterize hydrogel structure, biomechanical, degradation properties, and tECM release kinetics, FTIR, tensile tests, ex vivo hydrogel degradation, SEM and ex vivo tECM protein release kinetics assay were performed, respectively, as previously described (Experimental Section, Supporting Information).

Encapsulation of ASCs in TenoGel: hASCs were isolated from the infrapatellar fat pad tissue obtained from patients undergoing total knee arthroplasty, following the previously established protocols and in accordance with approved guidelines from The Chinese University of Hong Kong Institutional Review Board.[47] The isolated cells were further sorted using an human MSC analysis kit (BD Biosciences) with positive markers

including CD90, CD105, CD73, and CD44, and negative markers including CD34, CD11b, CD19, CD45, and HLA-DR. The cells were then subjected to colony-forming unit-fibroblast (CFU-F) and tri-lineage differentiation assays until passage 7 as previously described. hASCs from passages 4–7 were used in the current study.

To encapsulated hASCs within TenoGel supplemented with tECM, hASCs at a concentration of 6×10^6 cells mL^{-1} were mixed with GelMA/OA pre-polymer containing tECM (final concentration: 1.5 mg mL^{-1}) and followed the gelation procedures described in the Experimental Section (Supporting Information). Additionally, to apply mechanical stimulation to hASCs within TenoGel, as-fabricated cell-hydrogel constructs (≈135 µL per gel; 35 mm length × 3.5 mm width × 1.07 mm thickness) were cultured statically for ≈12 h to allow encapsulated cells settle down in hydrogels before being subjected to uniaxial tensile loading. The uniaxial tensile loading was performed using a commercial bioreactor (MCT6, CellScale biomaterials testing, Canada) with the following regimens: 8% strain, applied at a frequency of 0.5 Hz, for 6 h per day.

To simulate the principal stress distribution in the cell-hydrogel constructs undergoing uniaxial 8% stretching in the bioreactor, FEA was performed using commercially available software (COMSOL Multiphysics 6.0; COMSOL Inc., Sweden) as previously described.[110] Briefly, the hydrogel (35 mm (length) × 3.5 mm (width) × 1.07 mm (thickness)) and embedded cell-like component (diameter: 10 µm) were treated as isotropic hyperelastic solids, with elastic moduli obtained from experimental measurement and literature (230 kPa for GelMA/OA hydrogel and 2 kPa for human stem cells).[111] A Poisson's ratio of 0.5 was used for both hydrogel and embedded cell-like components.

RNA-seq Analysis of hASCs-TenoGel In Vitro: RNA-Seq analysis was conducted to explore the transcriptomic characterization of hASCs culturing in different TenoGel groups. Specifically, four experimental groups were established, 1) "Gel (Ctrl)": hASCs within GelMA/OA hydrogel in static culture; 2) "TenoGel (Loading)": hASCs within GelMA/OA hydrogel in uniaxial tensile loading culture; 3) "TenoGel (tECM)": hASCs within tECM containing-GelMA/OA hydrogel in static culture; and 4) "TenoGel (tECM+Loading)": hASCs within tECM containing-GelMA/OA hydrogel in uniaxial tensile loading culture. At designed time points (day 6, 10, and 21), total RNA from hASCs in hydrogel constructs were isolated for further bioinformatics analysis. Specifically, the cell-hydrogel constructs were collected and transferred into Eppendorf tubes containing 500 µL TRIzol (Invitrogen), and then homogenized in liquid nitrogen to ensure complete lysis and extraction of RNA by TRIzol (Experimental Section, Supporting Information).[112]

The gene expression analysis was carried out using an in-house pipeline and open-source R packages (v. 3.6.1, http://www.r-project.org/) as previously described (Experimental Section, Supporting Information).[19] The sequencing datasets were further analyzed as follows: (1) Principle component analysis (PCA) was performed using the *plotPCA* function of *DESeq2* packages[113]; (2) DEGs between hASCs cultured in two different TenoGel designs were estimated by the *Wald* test function in *DESeq2*. DEGs were identified as genes with > 2-fold change and false discovery rate (FDR) < 0.05 and further visualized by Venn gram as well as heatmap. The DEG heatmap displayed the top 20 upregulated and top 20 downregulated DEGs in the comparison of TenoGel (Loading)/(tECM)/(tECM+Loading) versus Gel (Ctrl) at respective time point; (3) To understand how different TenoGel designs influence the tenogenic and osteogenic differentiation of hASCs, 30 well-established marker genes associated with tenogenesis, and osteogenesis, were first selected including *COL11A1*, *COL1A1*, *COL3A1*, *COL5A1*, *COMP*, *DCN*, *EGR1*, *EYA2*, *FMOD*, *LUM*, *MKX*, *POSTN*, *SCX*, *TGFB3*, *TNC*, *TNMD* for tenogenesis and *ALPL*, *BGLAP*, *BMP2*, *BMPR1A*, *BMPR1B*, *CAMK2N1*, *CKB*, *CRYAB*, *GPNMB*, *OPTN*, *RUNX2*, *SMAD3*, *STAT1*, *SPP1* for osteogenesis. The expression of these genes was extracted using the filter function in the R package tidyverse and further visualized using heatmaps. ssGSEA was further used to evaluate the enrichment scores of each sample on hASCs tenogeneic and osteogenic differentiation, based on above listed marker genes, using the *GSVA* R package; (4) GSEA(v. 4.1.0, https://www.gsea-msigdb.org/gsea/index.jsp) was performed to examine the enrichment of "tenocyte" gene set from the TISSUES 2.0 database (available at https://tissues.jensenlab.org/Search).[54] The analysis specifically focused on comparing the TenoGel (tECM+Loading) group at day 10 with day 6, as well as day 21 with day 10. Gene sets were considered significantly enriched if the absolute value of normalized enrichment score (NES) > 1, *p-value* < 0.05 and FDR< 0.25; (5) GO and the Kyoto Encyclopedia of Genes and Genomes (KEGG) pathway analysis were performed using enrichr (https://maayanlab.cloud/Enrichr/) (Experimental Section, Supporting Information).[114] GO terms or pathways were only considered significantly enriched if the FDR < 0.05 and REVIGO was employed to reduce redundant GO terms. Network analyses of identified pathways of interest were further performed using the Search Tool for Retrieval of Interacting Genes/Proteins (STRING, v. 11.5, http://geneontology.org) with high confidence (0.7),[115] and the results were visualized using Cytoscape software (v. 3.10.0, USA).[116] Additionally, time series analysis was conducted for the key genes identified in the selected significant pathways. The *vst* function in *DESeq2* was used to normalize the genes expression in each group and the line charts were generated using *ggplot2* R packages as well as GraphPad Prism software. 6) The gene expression levels of *IGF1*, *PDGFA*, *FGF2*, *ITGA5*, *ITGA11*, *ITGB1*, *PIK3CA*, *mTOR*, *FZD3*, *WNT5A* and *WNT7B* were measured, and the relative fold changes were calculated using the ΔΔCT method and normalized to the control group (Gel (Ctrl)) at designed time point. All primer sequences are listed in Table S3 (Supporting Information). For the WB analysis, the encapsulated hASCs were released by incubating the hydrogel constructs in a 1 mg mL^{-1} collagenase I solution for 1 h at 37 °C after 10 days of culturing.[117] The collected hASCs were then lysed, and the total proteins were extracted. The primary antibodies used were rabbit anti-p-Akt (Cell Signaling Technology, USA), rabbit anti-Akt (Cell Signaling Technology), rabbit anti-WNT5A (Thermo Fisher Scientific) and mouse anti-GAPDH (Abcam). The densitometry values of the bands were determined using ImageJ software (NIH), and the relative p-Akt/Akt and WNT5A were normalized to GAPDH.

Mathematical Model Construction: Mathematical models were further employed to assess and predict the potential relationships between TenoGel designs and the transcriptomic profiles of hASCs, focusing on tenogenic and osteogenic differentiation. Four different groups were included in the study as described in prior sections, which were "Gel (Ctrl)", "TenoGel (Loading)", "TenoGel (tECM)", and "TenoGel (tECM+Loading)". At designed time points (days 6, 10, and 21), total RNA was isolated and RNA-seq was performed as described earlier. As shown in Table S1 (Supporting Information), 81 canonical marker genes related to tenogenesis and osteogenesis were obtained based on the literature review. The marker gene expression profiles of hASCs were extracted using the filter function in the R package tidyverse. The AddModuleScore module in Seurat (version 4.0.5) was used to obtain the tenogenic and osteogenic differentiation scores of samples by calculating the average canonical marker gene expression levels of each cell type.[45] Subsequently, LR and RF were fit with tenogenic scores or osteogenic scores as the outcomes, and tECM supplementation and uniaxial tensile loading as the predictors. The RNA-seq dataset containing 36 samples was randomly and evenly split into 3 disjoint sets for 3-fold CV. The performance of LR and RF were evaluated using each fold as the validation set once and the remaining sets as the training sets. Each sample in the dataset was described by 3 categorical features. Specifically, the presence or absence of tECM supplementation and uniaxial tensile loading were represented as binary features, while in vitro pre-conditioning day was coded as a categorical variable with 3 levels (day 6, day 10, and day 21). The specific machine learning and evaluation methods were as follows: (1) For the random forest model, the *randomForest* package was utilized in R. This non-linear machine learning method constructed an ensemble of decision trees and makes predictions by averaging their outputs. Different tree numbers were experimented with but found no significant difference in performance, so the default setting of 500 trees (Figure S6, Supporting Information) was used. To estimate feature importance, the *randomForest* package measured the performance drop before and after randomly permuting each feature; (2) For the linear regression model, the *lm()* function was used in R (v4.1.3) to fit separate models for each split. The features were encoded using dummy encodings. In each of the 3 splits, a separate LR model was fitted using the training splits and evaluated on

the validation split. After confirming satisfactory model performance for either tenogenic or osteogenic scores, a final LR model was fitted using all 36 data points for interpretation. The coefficients and p-values were obtained using the *summary()* function in R for interpretation; (3) To comprehensively evaluate the performance of the models, 2 standard performance metrics, namely mean squared error (MSE) and R-squared (R) were implemented, which are defined as follows (Equations (1) and (2)):

$$\mathrm{MSE} = \frac{1}{n}\sum_{i=1}^{n}(y_i - \hat{y}_i)^2 \tag{1}$$

$$\mathrm{R}^2 = 1 - \frac{\sum_{i=1}^{n}(y_i - \hat{y}_i)^2}{\sum_{i=1}^{n}(y_i - \bar{y})^2} \tag{2}$$

where n is the number of samples. y_i is the true outcome of sample x_i, $\hat{y}_i$ is the predicted outcome of sample x_i, and $\bar{y} = \frac{1}{n}\sum_{i=1}^{n} y_i$. While R^2 measures are not generally used for evaluating non-linear regression models since the definition of proportionate reduction in variation may no longer stand, it should be noted that R^2 measure is completely acceptable when used for comparing the same or nested non-linear models.[118]

Characterization of Pre-Conditioned, Human ASCs-TenoGel In Vitro: A set of experiments were performed to characterize the viability, metabolism, morphology, tenogenic differentiation, mineralization, and senescence of hASCs encapsulated within TenoGels as described in Experimental Section (Supporting Information). The nanoindentation test was performed to characterize the micromechanical properties of the hASCs-encapsulated TenoGel constructs (Experimental Section, Supporting Information).

Characterization of the Efficacy of In Vitro Preconditioned, rASCs-TenoGel for Tendon Repair: Similarly, as hASCs-TenoGel construct preparation, rASCs (passage 3–4, Cyagen Biosciences, USA) at a concentration of 6×10^6 cells mL^{-1} were pre-conditioned within TenoGel in vitro prior to in vivo implantation. rASCs instead of human ASCs were preconditioned in TenoGels to avoid severe immune response. To assess mineralization of rASCs-TenoGel in vitro, rASCs were encapsulated within Gel only, as well as various TenoGel groups, and ARS staining was performed (Experimental Section, Supporting Information). To investigate the tendon healing efficacy of rASCs preconditioned in TenoGel, a rat patellar tendon injury model was established as similarly described.[107] All animal experiments of Sprague-Dawley rats (10–12 weeks old; 300–400 g body weight; The Laboratory Animal Services Centre, The Chinese University of Hong Kong) were conducted in accordance with the Animal Experimentation Ethics Committee from The Chinese University of Hong Kong. Briefly, animals were anaesthetized with isoflurane (2 −2.5 vol.%) while a full-thickness, central window defects (1 mm (width) × 4 mm (length)) were created between the distal patella and tibial tuberosity as shown in Figure 7A. Four groups were prepared: (1) Defect only group: the tendon defects were created without hydrogel implantation; (2) Gel only group: cell-free GelMA/OA hydrogels were implanted into the tendon defects; (3) rASCs-Gel (Ctrl) group: rASCs were seeded into the GelMA/OA control hydrogels without tECM supplementation and static cultured for 10 days in basic culture medium (Cyagen Biosciences); and (4) rASCs-TenoGel (tECM+Loading) group: rASCs were seeded in the tECM supplemented GelMA/OA hydrogels and mechanically preconditioned (8% strain at a frequency of 0.5 Hz for 6 h per day) for 10 days in basic culture medium (Cyagen Biosciences). Hydrogel constructs of different groups (7 mm (length) × 3.5 mm (width) × 1.07 mm (thickness)) were placed on the tendon defects and secured by sutures (4–0) as shown in Figure 7A. The wound was closed in layers after surgery. The animals received buprenorphine (0.05 mg kg^{-1}, Buprenex) subcutaneously for 3 days and returned to free cage activity. A total of 68 rats underwent the surgical procedure, with the detailed distribution among each group as described in the figure legend. The uninjured tendons on the contralateral side were designated as the intact control (intact ctrl) for comparative analysis. Additionally, a mock surgery in rat cadavers was further performed to demonstrate the potential application of TenoGel for the treatment of tendon complete ruptures (Experimental Section, Supporting Information).

To examine the retention and survival of rASCs after implantation, in vivo imaging was performed as previously described with modification (Experimental Section, Supporting Information).[90] At designed time points, rat patellar tendons were harvested for macroscopic, histological, and biomechanical evaluations as follows: (1) To assess morphological properties of regenerated tendons, the length, width, and thickness of each group were measured in situ using digital callipers (Mitutoyo Corp, Japan) as shown in Figure 7C. The patellar tendon length was defined as the distance from the distal apex of the patellar to the deep insertion at the tibial tuberosity[119]; (2) For histological analyses, paraffined-embedded tissue sections (5 µm) were stained with H&E, Picrosirius red, Alcian blue, Safranin O, and Von Kossa. The stained sections were digitally captured using a Nikon microscope (Ni-U Eclipse Upright Microscope) or a polarizing microscope (Nikon Ni-U Eclipse Upright Microscope equipped with D-SA Analyzer Slide for Simple Polarization) and performed the semi-quantification analysis (Experimental Section, Supporting Information); (3) To perform biomechanical testing, tissue samples were harvested specifically from the tendon-patella and tendon-tibia composite after dissecting the rat knee. To perform the biomechanical test, tissue samples were harvested specifically from the tendon-patella and tendon-tibia composite after dissecting the rat knee. All harvested specimens were wrapped in gauze soaked in buffered saline and stored at −20 °C prior to testing. A horizontal mechanical tester (Admet, eXpert 4000, USA) equipped with a 100 lb load cell was used in conjunction with MTestQuattro Software (Admet, Version 6.00.05) to acquire tensile data. The specimens were secured with the patellar bone gripped using a sandpaper and the tibia mounted in a custom-made holder as shown in Figure 7D. The specimens were preloaded to 0.1 N and subsequently uniaxially loaded at a rate of 0.5 mm s^{-1}, corresponding to a strain rate of ≈1% s^{-1}, until failure. The mechanical properties of the healed tendons including stiffness (N/mm), failure force (N), tensile modulus (MPa), and stress at failure (MPa) were calculated.

Statistical Analysis: Statistical analyses were performed using GraphPad Prism software (Version 8.2.1, USA). All experiments were performed with at least three replicates per group and quantitative data were presented as mean ± standard error of the mean (mean ± SEM) or mean ± standard deviation (mean ± SD) as the figure legend described. Sample sizes are noted in figure legends. One-way ANOVA with post-hoc Tukey's multiple comparisons was conducted where appropriate. p values less than 0.05 ($p < 0.05$) were considered to be statistically significant as indicated (*; $p < .05$, **; $p < .01$, and ***; $p < .001$).

Supporting Information

Supporting Information is available from the Wiley Online Library or from the author.

Acknowledgements

This work was supported by the Research Grants Council of Hong Kong SAR (GRF 14121121 Award and 14118620 Award, D.M.W.; Early Career Scheme Award 24201720 and GRF 14213922 Award, D.F.E.K.), The National Natural Science Foundation of China (NSFC)/Research Grants Council (RGC) of Hong Kong Joint Research Scheme (CUHK409/23, D.M.W.), The Innovation and Technology Commission of Hong Kong SAR (Health@InnoHK, D.M.W., R.S.T., D.F.E.K.), and the Lee Quo Wei and Lee Yick Hoi Lun Professorship of Tissue Engineering and Regenerative Medicine (R.S.T.).

Conflict of Interest

The authors declare no conflict of interest.

Data Availability Statement

The data that support the findings of this study are available from the corresponding author upon reasonable request.

Keywords

extracellular matrix, hydrogel, materiomics, stem cell therapy, tendon regeneration

Received: December 15, 2023
Revised: September 4, 2024
Published online: October 17, 2024

[1] P. Sharma, N. Maffulli, *J. Bone Jt. Surg. Am. Vol.* **2005**, *87*, 187.
[2] N. L. Millar, K. G. Silbernagel, K. Thorborg, P. D. Kirwan, L. M. Galatz, G. D. Abrams, G. A. C. Murrell, I. B. McInnes, S. A. Rodeo, *Nat. Rev. Dis. Primers* **2021**, *7*, 1.
[3] G. Chamberlain, J. Fox, B. Ashton, J. Middleton, *Stem Cells* **2007**, *25*, 2739.
[4] I. Mastrolia, E. M. Foppiani, A. Murgia, O. Candini, A. V. Samarelli, G. Grisendi, E. Veronesi, E. M. Horwitz, M. Dominici, *Stem Cells Transl. Med.* **2019**, *8*, 1135.
[5] P. P. Lui, Y. C. Cheuk, Y. W. Lee, K. M. Chan, *J. Orthop. Res.* **2012**, *30*, 37.
[6] J. Hu, S. Liu, C. Fan, *Front. Bioeng. Biotechnol.* **2023**, *11*, 1135090.
[7] B. R. Freedman, D. J. Mooney, *Adv. Mater.* **2019**, *31*, 1806695.
[8] B. Shiroud Heidari, R. Ruan, E. Vahabli, P. Chen, E. M. De-Juan-Pardo, M. Zheng, B. Doyle, *Bioact. Mater.* **2023**, *19*, 179.
[9] G. Yang, B. B. Rothrauff, H. Lin, R. Gottardi, P. G. Alexander, R. S. Tuan, *Biomaterials* **2013**, *34*, 9295.
[10] K. Li, X. Zhang, D. Wang, R. S. Tuan, D. F. E. Ker, *Biomater. Adv.* **2023**, *146*, 213316.
[11] Y. Morita, S. Watanabe, Y. Ju, B. Xu, *Acta Bioeng. Biomech.* **2013**, *15*, 71.
[12] C. K. Kuo, R. S. Tuan, *Tissue Eng. Part A* **2008**, *14*, 1615.
[13] D. Wang, D. F. E. Ker, K. W. Ng, K. Li, B. Gharaibeh, M. Safran, E. Cheung, P. Campbell, L. Weiss, Y. P. Yang, *NPG Asia Mater.* **2021**, *13*, 26.
[14] R. Sheng, J. Liu, W. Zhang, Y. Luo, Z. Chen, J. Chi, Q. Mo, M. Wang, Y. Sun, C. Liu, Y. Zhang, Y. Zhu, B. Kuang, C. Yan, H. Liu, L. J. Backman, J. Chen, *Adv. Sci. (Weinh)* **2023**, *10*, 2206814.
[15] G. Chu, Z. Yuan, C. Zhu, P. Zhou, H. Wang, W. Zhang, Y. Cai, X. Zhu, H. Yang, B. Li, *Acta Biomater.* **2019**, *92*, 254.
[16] Z. Wang, W. J. Lee, B. T. H. Koh, M. Hong, W. Wang, P. N. Lim, J. Feng, L. S. Park, M. Kim, E. S. Thian, *Sci. Adv.* **2018**, *4*, aat4537.
[17] H. R. Screen, D. E. Berk, K. E. Kadler, F. Ramirez, M. F. Young, *J. Orthop. Res.* **2015**, *33*, 793.
[18] B. B. Rothrauff, G. Yang, R. S. Tuan, *Stem Cell Res. Ther.* **2017**, *8*, 133.
[19] Y. Rao, C. Zhu, H. C. Suen, S. Huang, J. Liao, D. F. E. Ker, R. S. Tuan, D. Wang, *Stem Cell Res. Ther.* **2022**, *13*, 380.
[20] S. Huang, Y. Rao, A. L. Ju, D. F. E. Ker, A. M. Blocki, D. M. Wang, R. S. Tuan, *Acta Biomater.* **2024**, *176*, 99.
[21] K. Spanoudes, D. Gaspar, A. Pandit, D. I. Zeugolis, *Trends Biotechnol.* **2014**, *32*, 474.
[22] M. T. Galloway, A. L. Lalley, J. T. Shearn, *J. Bone Jt. Surg. Am.* **2013**, *95*, 1620.
[23] T. Wang, P. Chen, M. Zheng, A. Wang, D. Lloyd, T. Leys, Q. Zheng, M. H. Zheng, *J. Orthop. Res.* **2018**, *36*, 566.
[24] S. Y. Wu, W. Kim, T. J. Kremen Jr., *Front. Bioeng. Biotechnol.* **2022**, *10*, 826748.
[25] I. Donderwinkel, R. S. Tuan, N. R. Cameron, J. E. Frith, *J. Orthop. Transl.* **2023**, *43*, 1.
[26] J. Burk, A. Plenge, W. Brehm, S. Heller, B. Pfeiffer, C. Kasper, *Stem Cells Int.* **2016**, *2016*, 7342379.
[27] C. Rinoldi, A. Fallahi, I. K. Yazdi, J. Campos Paras, E. Kijeńska-Gawrońska, G. Trujillo-de Santiago, A. Tuoheti, D. Demarchi, N. Annabi, A. Khademhosseini, W. Swieszkowski, A. Tamayol, *ACS Biomater. Sci. Eng.* **2019**, *5*, 2953.
[28] C. Rinoldi, M. Costantini, E. Kijeńska-Gawrońska, S. Testa, E. Fornetti, M. Heljak, M. Ćwiklińska, R. Buda, J. Baldi, S. Cannata, J. Guzowski, C. Gargioli, A. Khademhosseini, W. Swieszkowski, *Adv. Healthcare Mater.* **2019**, *8*, 1801218.
[29] S. W. Cranford, J. de Boer, C. van Blitterswijk, M. J. Buehler, *Adv. Mater.* **2013**, *25*, 802.
[30] B. Basu, N. H. Gowtham, Y. Xiao, S. R. Kalidindi, K. W. Leong, *Acta Biomater.* **2022**, *143*, 1.
[31] P. K. Nguyen, D. Nag, J. C. Wu, *Adv. Drug Delivery Rev.* **2010**, *62*, 1175.
[32] D. Gaspar, K. Spanoudes, C. Holladay, A. Pandit, D. Zeugolis, *Adv. Drug Delivery Rev.* **2015**, *84*, 240.
[33] Y. Li, M. Ramcharan, Z. Zhou, D. J. Leong, T. Akinbiyi, R. J. Majeska, H. B. Sun, *Sci. Rep.* **2018**, *8*, 16377.
[34] P. P. Lui, *J. Cell. Mol. Med.* **2013**, *17*, 55.
[35] A. K. Levay, J. D. Peacock, Y. Lu, M. Koch, R. B. Hinton Jr., K. E. Kadler, J. Lincoln, *Circ. Res.* **2008**, *103*, 948.
[36] Y. Yoshimoto, A. Takimoto, H. Watanabe, Y. Hiraki, G. Kondoh, C. Shukunami, *Sci. Rep.* **2017**, *7*, 45010.
[37] P. Sarmiento, D. Little, *NPJ Regener. Med.* **2021**, *6*, 61.
[38] H. A. Awad, G. P. Boivin, M. R. Dressler, F. N. Smith, R. G. Young, D. L. Butler, *J. Orthop. Res.* **2003**, *21*, 420.
[39] B. R. Freedman, D. J. Mooney, E. Weber, *Sci. Transl. Med.* **2022**, *14*, abl8814.
[40] A. L. Kersey, T.-U. Nguyen, B. Nayak, I. Singh, A. K. Gaharwar, *Mater. Today* **2023**, *64*, 98.
[41] A. P. Liu, E. A. Appel, P. D. Ashby, B. M. Baker, E. Franco, L. Gu, K. Haynes, N. S. Joshi, A. M. Kloxin, P. H. J. Kouwer, J. Mittal, L. Morsut, V. Noireaux, S. Parekh, R. Schulman, S. K. Y. Tang, M. T. Valentine, S. L. Vega, W. Weber, N. Stephanopoulos, O. Chaudhuri, *Nat. Mater.* **2022**, *21*, 390.
[42] M. Darnell, A. O'Neil, A. Mao, L. Gu, L. L. Rubin, D. J. Mooney, *Proc. Natl. Acad. Sci. USA* **2018**, *115*, E8368.
[43] N. Groen, H. Yuan, D. G. Hebels, G. Koçer, F. Mbuyi, V. LaPointe, R. Truckenmüller, C. A. van Blitterswijk, P. Habibović, J. de Boer, *Adv. Mater.* **2017**, *29*, 1603259.
[44] J. E. Frith, G. D. Kusuma, J. Carthew, F. Li, N. Cloonan, G. A. Gomez, J. J. Cooper-White, *Nat. Commun.* **2018**, *9*, 257.
[45] Y. Zhou, X. Ping, Y. Guo, B. C. Heng, Y. Wang, Y. Meng, S. Jiang, Y. Wei, B. Lai, X. Zhang, X. Deng, *Adv. Mater.* **2023**, *35*, 2210637.
[46] O. Jeon, J.-Y. Shin, R. Marks, M. Hopkins, T.-H. Kim, H.-H. Park, E. Alsberg, *Chem. Mater.* **2017**, *29*, 8425.
[47] D. Wang, C. C. M. Pun, S. Huang, T. C. M. Tang, K. K. W. Ho, B. B. Rothrauff, P. S. H. Yung, A. M. Blocki, E. D. F. Ker, R. S. Tuan, *FASEB J.* **2020**, *34*, 8172.
[48] F. Brandl, F. Sommer, A. Goepferich, *Biomaterials* **2007**, *28*, 134.
[49] J. L. Drury, D. J. Mooney, *Biomaterials* **2003**, *24*, 4337.
[50] L. Han, L. Yan, K. Wang, L. Fang, H. Zhang, Y. Tang, Y. Ding, L.-T. Weng, J. Xu, J. Weng, Y. Liu, F. Ren, X. Lu, *NPG Asia Mater.* **2017**, *9*, 372.
[51] J. Seo, J. Y. Shin, J. Leijten, O. Jeon, A. Bal Öztürk, J. Rouwkema, Y. Li, S. R. Shin, H. Hajiali, E. Alsberg, A. Khademhosseini, *ACS Appl. Mater. Interfaces* **2018**, *10*, 13293.
[52] K. Sakthivel, H. Kumar, M. G. A. Mohamed, B. Talebjedi, J. Shim, H. Najjaran, M. Hoorfar, K. Kim, *Small* **2020**, *16*, 2000941.
[53] G. Merolla, S. Singh, P. Paladini, G. Porcellini, *J. Orthop. Traumatol.* **2016**, *17*, 7.
[54] O. Palasca, A. Santos, C. Stolte, J. Gorodkin, L. J. Jensen, *Database (Oxford)* **2018**, *2018*, bay003.
[55] T. Wang, C. Thien, C. Wang, M. Ni, J. Gao, A. Wang, Q. Jiang, R. S. Tuan, Q. Zheng, M. H. Zheng, *FASEB J.* **2018**, *32*, 4804.
[56] S. K. Theodossiou, J. B. Murray, L. A. Hold, J. M. Courtright, A. M. Carper, N. R. Schiele, *Stem Cell Res. Ther.* **2021**, *12*, 88.

[57] K. Lu, H. Tang, Y. Wang, L. Wang, M. Zhou, G. He, H. Lu, C. Tang, W. Chen, X. Ma, K. Tang, Z. Deng, *Stem Cells Int.* **2023**, *2023*, 2915826.
[58] Y. Li, T. Wu, S. Liu, *Front. Cell Dev. Biol.* **2021**, *9*, 629515.
[59] M. W. Hast, A. Zuskov, L. J. Soslowsky, *Bone Jt. Res.* **2014**, *3*, 193.
[60] P. P. Lui, *Stem Cells Cloning* **2015**, *8*, 163.
[61] A. E. C. Nichols, K. T. Best, A. E. Loiselle, *Transl. Res.* **2019**, *209*, 156.
[62] S. P. Lake, J. G. Snedeker, V. M. Wang, H. Awad, H. R. C. Screen, S. Thomopoulos, *J. Orthop. Res.* **2023**, *41*, 2105.
[63] B. R. Freedman, A. Kuttler, N. Beckmann, S. Nam, D. Kent, M. Schuleit, F. Ramazani, N. Accart, A. Rock, J. Li, M. Kurz, A. Fisch, T. Ullrich, M. W. Hast, Y. Tinguely, E. Weber, D. J. Mooney, *Nat. Biomed. Eng.* **2022**, *6*, 1167.
[64] E. S. Dragan, *Chem. Eng. J.* **2014**, *243*, 572.
[65] Z. Xu, Y. Fang, Y. Chen, Y. Zhao, W. Wei, C. Teng, *Front. Bioeng. Biotechnol.* **2022**, *10*, 851660.
[66] R. Dang, L. Chen, F. Sefat, X. Li, S. Liu, X. Yuan, X. Ning, Y. S. Zhang, P. Ji, X. Zhang, *Small* **2022**, *18*, 2105255.
[67] L. Du, J. Wu, Y. Han, C. Wu, *Sci. Adv.* **2024**, *10*, adk6610.
[68] Z. Chen, B. Zhou, X. Wang, G. Zhou, W. Zhang, B. Yi, W. Wang, W. Liu, *Acta Biomater.* **2022**, *145*, 297.
[69] A. Subramanian, L. F. Kanzaki, J. L. Galloway, T. F. Schilling, *Elife* **2018**, *7*, e38069.
[70] M. Benjamin, E. Kaiser, S. Milz, *J. Anat.* **2008**, *212*, 211.
[71] H. Y. Nam, B. Pingguan-Murphy, A. A. Abbas, A. M. Merican, T. Kamarul, *Stem Cells Int.* **2019**, *2019*, 1.
[72] P. K. Nguyen, F. Deng, S. Assi, P. Paco, S. Fink, C. Stockwell, C. K. Kuo, *J. Orthop. Res.* **2022**, *40*, 1584.
[73] V. Miceli, M. Bulati, G. Iannolo, G. Zito, A. Gallo, P. G. Conaldi, *Int. J. Mol. Sci.* **2021**, *22*, 763.
[74] Y. Xu, S. Dong, Q. Zhou, X. Mo, L. Song, T. Hou, J. Wu, S. Li, Y. Li, P. Li, Y. Gan, J. Xu, *Biomaterials* **2014**, *35*, 2760.
[75] B. Zhang, Q. Luo, B. Deng, Y. Morita, Y. Ju, G. Song, *Acta Biomater.* **2018**, *74*, 247.
[76] M. Kongsgaard, V. Kovanen, P. Aagaard, S. Doessing, P. Hansen, A. H. Laursen, N. C. Kaldau, M. Kjaer, S. P. Magnusson, *Scand. J. Med. Sci. Sports* **2009**, *19*, 790.
[77] A. S. Agergaard, R. B. Svensson, R. Hoeffner, P. Hansen, C. Couppé, M. Kjaer, S. P. Magnusson, *Scand J Med Sci Sports* **2021**, *31*, 1981.
[78] H. Zhang, Y. Chen, C. Fan, R. Liu, J. Huang, Y. Zhang, C. Tang, B. Zhou, X. Chen, W. Ju, Y. Zhao, J. Han, P. Wu, S. Zhang, W. Shen, Z. Yin, X. Chen, H. Ouyang, *Biomaterials* **2022**, *280*, 121238.
[79] A. A. Hussien, B. Niederoest, M. Bollhalder, N. Goedecke, J. G. Snedeker, *Adv. Healthcare Mater.* **2023**, *12*, 2101216.
[80] D. A. Kaji, A. M. Montero, R. Patel, A. H. Huang, *Nat. Commun.* **2021**, *12*, 4208.
[81] N. P. Disser, K. B. Sugg, J. R. Talarek, D. C. Sarver, B. J. Rourke, C. L. Mendias, *FASEB J.* **2019**, *33*, 12680.
[82] C. I. Lorda-Diez, J. A. Montero, J. A. Garcia-Porrero, J. M. Hurle, *ACS Chem. Biol.* **2014**, *9*, 72.
[83] E. Havis, M. A. Bonnin, I. Olivera-Martinez, N. Nazaret, M. Ruggiu, J. Weibel, C. Durand, M. J. Guerquin, C. Bonod-Bidaud, F. Ruggiero, R. Schweitzer, D. Duprez, *Development* **2014**, *141*, 3683.
[84] Y. Jiang, H. Liu, H. Li, F. Wang, K. Cheng, G. Zhou, W. Zhang, M. Ye, Y. Cao, W. Liu, H. Zou, *Biomaterials* **2011**, *32*, 4085.
[85] Y. Liu, C. W. Suen, J. F. Zhang, G. Li, *J. Orthop. Transl.* **2017**, *9*, 28.
[86] S. Freeman, S. Calabro, R. Williams, S. Jin, K. Ye, *Front. Bioeng. Biotechnol.* **2022**, *10*, 913579.
[87] I. Donderwinkel, R. S. Tuan, N. R. Cameron, J. E. Frith, *Acta Biomater.* **2022**, *145*, 25.
[88] S. M. McDonald, E. K. Augustine, Q. Lanners, C. Rudin, L. Catherine Brinson, M. L. Becker, *Nat. Commun.* **2023**, *14*, 4838.
[89] M. S. Rehmann, J. I. Luna, E. Maverakis, A. M. Kloxin, *J. Biomed. Mater. Res. A* **2016**, *104*, 1162.
[90] T. Nakajima, A. Nakahata, N. Yamada, K. Yoshizawa, T. M. Kato, M. Iwasaki, C. Zhao, H. Kuroki, M. Ikeya, *Nat. Commun.* **2021**, *12*, 5012.
[91] S. A. Rodeo, D. Delos, R. J. Williams, R. S. Adler, A. Pearle, R. F. Warren, *Am. J. Sports Med.* **2012**, *40*, 1234.
[92] H. A. Awad, D. L. Butler, G. P. Boivin, F. N. Smith, P. Malaviya, B. Huibregtse, A. I. Caplan, *Tissue Eng.* **1999**, *5*, 267.
[93] S. A. Abbah, K. Spanoudes, T. O'Brien, A. Pandit, D. I. Zeugolis, *Stem Cell Res. Ther.* **2014**, *5*, 38.
[94] D. Dey, J. Bagarova, S. J. Hatsell, K. A. Armstrong, L. Huang, J. Ermann, A. J. Vonner, Y. Shen, A. H. Mohedas, A. Lee, E. M. Eekhoff, A. van Schie, M. B. Demay, C. Keller, A. J. Wagers, A. N. Economides, P. B. Yu, *Sci. Transl. Med.* **2016**, *8*, 366ra163.
[95] X. Wang, F. Li, L. Xie, J. Crane, G. Zhen, Y. Mishina, R. Deng, B. Gao, H. Chen, S. Liu, P. Yang, M. Gao, M. Tu, Y. Wang, M. Wan, C. Fan, X. Cao, *Nat. Commun.* **2018**, *9*, 551.
[96] T. Tengman, J. Riad, *Orthop. J. Sports Med.* **2013**, *1*, 232596711350473.
[97] P. P. Lui, O. T. Wong, Y. W. Lee, *Cytotherapy* **2016**, *18*, 99.
[98] Z. Yin, J. Guo, T. Y. Wu, X. Chen, L. L. Xu, S. E. Lin, Y. X. Sun, K. M. Chan, H. Ouyang, G. Li, *Stem Cells Transl. Med.* **2016**, *5*, 1106.
[99] V. S. Nirmalanandhan, N. Juncosa-Melvin, J. T. Shearn, G. P. Boivin, M. T. Galloway, C. Gooch, G. Bradica, D. L. Butler, *Tissue Eng. Part A* **2009**, *15*, 2103.
[100] A. S. Vasilevich, A. Carlier, J. de Boer, S. Singh, *Trends Biotechnol.* **2017**, *35*, 743.
[101] G. Subramanian, A. Stasuk, M. Elsaadany, E. Yildirim-Ayan, *Stem Cells Int.* **2017**, *2017*, 1.
[102] E. Bianchi, A. Faccendini, E. Del Favero, C. Ricci, L. Caliogna, B. Vigani, F. C. Pavesi, C. Perotti, R. M. A. Domingues, M. E. Gomes, S. Rossi, G. Sandri, *Pharmaceutics* **2022**, *14*, 2153.
[103] S. Qian, Z. Wang, Z. Zheng, J. Ran, J. Zhu, W. Chen, *Med. Sci. Monit.* **2019**, *25*, 269.
[104] A. Islam, T. Mbimba, M. Younesi, O. Akkus, *Acta Biomater.* **2017**, *58*, 244.
[105] B. R. Freedman, R. S. Knecht, Y. Tinguely, G. E. Eskibozkurt, C. S. Wang, D. J. Mooney, *Acta Biomater.* **2022**, *143*, 63.
[106] C. Liu, Q. Yu, Z. Yuan, Q. Guo, X. Liao, F. Han, T. Feng, G. Liu, R. Zhao, Z. Zhu, H. Mao, C. Zhu, B. Li, *Bioact. Mater.* **2023**, *25*, 445.
[107] Y. Zhang, T. Lei, C. Tang, Y. Chen, Y. Liao, W. Ju, H. Zhang, B. Zhou, R. Liang, T. Zhang, C. Fan, X. Chen, Y. Zhao, Y. Xie, J. Ye, B. C. Heng, X. Chen, Y. Hong, W. Shen, Z. Yin, *Biomaterials* **2021**, *271*, 120722.
[108] L. Yang, S. Pijuan-Galito, H. S. Rho, A. S. Vasilevich, A. D. Eren, L. Ge, P. Habibović, M. R. Alexander, J. de Boer, A. Carlier, P. van Rijn, Q. Zhou, *Chem. Rev.* **2021**, *121*, 4561.
[109] K. M. Chan, S. C. Fu, *Sports Med. Arthrosc. Rehabil. Ther. Technol.* **2009**, *1*, 23.
[110] M. Govoni, C. Muscari, J. Lovecchio, C. Guarnieri, E. Giordano, *Stem Cell Rev. Rep.* **2016**, *12*, 189.
[111] N. I. Nikolaev, T. Müller, D. J. Williams, Y. Liu, *J. Biomech.* **2014**, *47*, 625.
[112] A. Gasparian, L. Daneshian, H. Ji, E. Jabbari, M. Shtutman, *Anal. Biochem.* **2015**, *484*, 1.
[113] M. I. Love, W. Huber, S. Anders, *Genome Biol.* **2014**, *15*, 550.
[114] M. V. Kuleshov, M. R. Jones, A. D. Rouillard, N. F. Fernandez, Q. Duan, Z. Wang, S. Koplev, S. L. Jenkins, K. M. Jagodnik, A. Lachmann, M. G. McDermott, C. D. Monteiro, G. W. Gundersen, A. Ma'ayan, *Nucleic Acids Res.* **2016**, *44*, W90.
[115] D. Szklarczyk, A. L. Gable, D. Lyon, A. Junge, S. Wyder, J. Huerta-Cepas, M. Simonovic, N. T. Doncheva, J. H. Morris, P. Bork, L. J. Jensen, C. V. Mering, *Nucleic Acids Res.* **2019**, *47*, D607.

[116] P. Shannon, A. Markiel, O. Ozier, N. S. Baliga, J. T. Wang, D. Ramage, N. Amin, B. Schwikowski, T. Ideker, *Genome Res.* **2003**, *13*, 2498.
[117] J. Sun, Y. T. Chan, K. W. K. Ho, L. Zhang, L. Bian, R. S. Tuan, Y. Jiang, *Bioact. Mater.* **2023**, *25*, 256.
[118] R. Anderson-Sprecher, *Am. Stat.* **1994**, *48*, 113.
[119] G. M. Hohenberger, M. Dreu, H. Kreuzthaler, G. Gruber, R. Riedl, A. Schwarz, I. Vielgut, H. Widhalm, P. Sadoghi, *Indian J. Orthop.* **2020**, *54*, 352.